PETROGRAPHIC AND PETROLOGICAL STUDY OF LUNAR ROCK MATERIALS

Stephen R. Winzer
Martin Marietta Corporation
Martin Marietta Laboratories
1450 South Rolling Road
Baltimore, Maryland 21227

May 1977
Final Report, May 5, 1976 - May 5, 1977

Prepared for
GODDARD SPACE FLIGHT CENTER
Greenbelt, Maryland 20771

TABLE OF CONTENTS

List of Figures

List of Tables

TECHNICAL REPORT STANDARD TITLE PAGE

1 Report No	2 Government Accession No	3 Recipient's Catalog No
4 Title and Subtitle Petrographic and Petrological Study of Lunar Rock Materials		5 Report Date May 20, 1977 6 Performing Organization Code
7 Author(s) Stephen R. Winzer		8 Performing Organization Report No
9 Performing Organization Name and Address Martin Marietta Laboratories 1450 S. Rolling Road Baltimore, Maryland 21227		10 Work Unit No 11 Contract or Grant No NAS5-23544
12. Sponsoring Agency Name and Address NASA Goddard Space Flight Center, Greenbelt, Maryland		13 Type of Report and Period Covered Final Report, May 5, 1976 - May 5, 1977 14 Sponsoring Agency Code
15 Supplementary Notes		

16. Abstract Impact melts and breccias from the Apollo 15 and 16 landing sites have been examined optically and by electron microscope/microprobe. Major and trace element abundances have been determined for selected samples. Apollo 16 breccias contain impact melts, metamorphic and primary igneous rocks. Metamorphic rocks may be the equivalents of the impact melts. Apollo 15 breccias studied are fragment-laden melts derived from gabbro and more basalt target rocks

Impact melts, breccias and tektites from Tenoumer, Dellen and Zhamanshin craters have been examined optically and by electron microscope/microprobe Major and trace elements, Rb/Sr and Sr isotopic abundances have been determined. Tenoumer melt crystallization histories are dependent on amount of fragmentary material included and composition. Mixing models cannot match both trace and major elements. Dellen melts are of unusual composition, and have crystallized relatively slowly from a hot melt. Zhamanshin impact melts are similar to basic Irghizites found in and near the crater, while siliceous Irghizites have no analog as yet in the impact melts.

17 Key Words (Selected by Author(s))	18 Distribution Statement
Petrography, Petrology, geochemistry, impact melts, breccias, impact craters, lunar samples 61175, 67455, 15255 Dellen, Tenoumer, Zhamanshin, Tektites	

19 Security Classif (of this report)	20 Security Classif (of this page)	21 No of Pages	22 Price*

*For sale by the Clearinghouse for Federal Scientific and Technical Information, Springfield, Virginia 22151

Figure 2. Technical Report Standard Title Page

PREFACE

Objective and scope of work

The objectives and scope of work performed under this contract were to examine, by optical and scanning electron microscope, and, where applicable, by transmission electron microscope and electron microprobe, lunar highlands breccias and terrestrial impact-generated breccias as designated by senior scientists at Goddard Space Flight Center. Appropriate samples were to be chosen for determination of large-ion-lithophile trace element abundances, major element abundances and Rb/Sr and Sr isotopic analysis. These data were to be reduced and interpreted, and, using the results as a guide, to initiate new work aimed at gaining further knowledge and understanding of the nature of, and processes forming, the lunar highlands crust, and surface processes affecting planets.

Conclusions

Samples, including chips, polished electron microprobe mounts and polished thin sections of samples from the Apollo 15 and 16 landing sites were examined and analyzed during the course of this study Major, minor and trace element analyses of lunar samples 15255, 67455 and 61175 have been completed. These data indicate that 15255 is a fragment-laden melt containing mineral and lithic fragments probably derived from mare basalts and gabbros By comparison with other lunar breccias and terrestrial impact melts and breccias, 15255 appears to be ejecta rather than part of a melt sheet. The breccia is coated with a vesicular glass rind which is similar in major element composition to the bulk breccia, but differs in

lithophile trace element composition. This rind was not derived from the host breccia.

61175 and 67455 are light-matrix, friable polymict breccias which contain clasts of melt rocks, anorthosite and metamorphic rocks (hornfelses and granulites). 61175 contains a highly varied suite of impact melts, granoblastic hornfelses, poikiloblastic hornfelses and granulites as well as a few shocked anorthosite clasts. 67455 contains a smaller variety of clasts, which include hornfelses of similar texture and composition to those in 61175, and a suite of hornfelses with higher Fe content. The anorthosites contain more plagioclase and have lower lithophile trace element abundances than the anorthosites in 61175. Study of these two rocks extends the presence of of the metamorphic component to two other sites at the Apollo 16 landing site, and suggests at least three stages of formation, including primary crystallization, thermal metamorphism and impact fusion.

Samples, including polished electron microprobe mounts, polished thin sections and hand specimens of impact melt and target rocks from three terrestrial meteorite impact craters have been examined and analyzed by electron microprobe for major elements and for lithophile trace elements, Rb/Sr and Sr isotopes. The Tenoumer and Dellen lake craters were found to have melts of unusual composition, which indicate different crystallization histories and cooling rates. Cooling rate and crystallization history are likely a function of both composition and the number of included fragments. Major element composition of Tenoumer melts can be explained by mixing amphibolite and granodiorite end members; however,trace element composition

cannot be so explained. An as yet unanalyzed component may be responsible for the trace element compositions of the melt.

Rocks from the Zhamanshin structure, near Aral, USSR, include shocked gneisses and siliceous limestones, impact melts of basaltic composition and dense black glasses (tektites) of siliceous and basaltic composition. Six samples have been separated and prepared for Rb/Sr and Sr isotopic analysis and determination of lithophile trace element abundances.

Recommendations

It is recommended that additional samples from 61175 be obtained and clasts separated for K/Ar, $^{40}Ar/^{39}Ar$, major element and trace element chemistry. Laser probe $^{40}Ar/^{39}Ar$ age dating should be undertaken on thoroughly characterized clasts. Further samples of glass coated breccias should be obtained from the Apollo 15 collection in order to analyze and compare 15255 with other glass-coated breccias from the Apollo 15 site.

Further samples of target and melt rocks should be obtained from the Dellen and Tenoumer craters for Rb/Sr and lithophile trace element analysis. These samples should be collected from the NE dike swarm at Tenoumer (not yet sampled) and from Norra and Sodra Dellen where impact melts different from those analyzed in this study have been found. Further samples of the Zhamanshin impact melts and their target rocks are being obtained from P. V. Florensky, and should be analyzed for Rb/Sr and Sr isotopes and lithophile trace element abundances Detailed petrographic and petrologic analysis should also be done on these melts

INTRODUCTION

As outlined in the statement of work under contract NAS5-23544, three areas of study were to be undertaken at the designation of senior GSFC scientists. These areas were: 1) Petrology and petrography of lunar rock materials, 2) Petrology and petrography, and isotopic analysis of terrestrial impactites and 3) Petrology and petrography of meteorites No meteorites were designated for study during this contract year, thus all work performed was done under 1 and 2.

The study of terrestrial meteorite impact craters as Lunar analogues is an important one as such studies provide primary data relating to the impact process. Such data can be applied directly, or can be used to interpret lunar breccias for which geological controls are lacking. This report presents results of detailed study of two terrestrial impact craters (Tenoumer, Mauritania and Dellen, Sweden), and preliminary results of studies of a third, the Zhamanshin structure in the USSR. The results of these studies, and others, provide a framework in which the returned lunar breccias can be understood. This report also presents the results of detailed studies of 61175, an Apollo 16 breccia which is the subject of an ongoing consortium study effort, and 15255, a glass-coated breccia from the Apollo 15 site.

PETROLOGY, PETROGRAPHY AND GEOCHEMISTRY OF TERRESTRIAL IMPACTITE

Introduction: Detailed studies of two terrestrial impact craters are nearing completion, while the other is undergoing detailed study at this time. These

three craters, Tenoumer in Mauritania, Dellen in Sweden and Zhamanshin in the USSR are all smaller craters (< 10 km in diameter) which contain impact melts. In this sense they differ from other small impact craters such as Odessa or Meteor Crater, which do not contain discrete bodies of melt, although glasses have been found associated with the latter craters. Of the four craters currently under study, Zhamanshin is unique in that it has associated with it a group of tektite-like glasses (Irghizites) (Florensky, 1975). Tenoumer crater has been the subject of extensive geochemical and isotopic studies for the past 2-1/2 years, and petrological studies of the melts have just been completed. The Dellen and Tenoumer structures are smaller craters which contain bodies of melt of unusual composition

TENOUMER CRATER, MAURITANIA

Tenoumer, at 1 9 km in diameter, is the smallest of the four craters studied It is located in the Sahara Desert about 250 km east of Zourat, Mauritania (Fudali, 1974) The crater was described by Richard-Molard (1948) and by Monod and Pomerol (1966). Both papers concluded that the crater was formed by volcanic processes. Later work by French et al. (1970) described features indicative of shock metamorphism in rocks from the crater providing strong evidence for the formation of the crater by meteorite impact. Further evidence, including the young age (2.5 my via K/Ar) and high initial Sr^{87}/Sr^{86} ratio (0.720) for the melt rocks, also suggested an impact origin. Fudali (1974) undertook a study of the impact melts found at Tenoumer, coming to the conclusion that these melts, which occur as dikelike bodies just outside the rim of the crater, were formed as a result of melting and mixing amphibolites and granodiorite, both of which are part of the

country rock suite. In Fudali's model, the dikes are formed by local melting of amphibolite which occurs as a dike striking through the center of the crater, and immediately adjacent granodiorite. This model differs somewhat from other models of melt formation in that the melts may be formed at some distance from the center of the crater, and the melts may not have the same composition everywhere in the crater.

Because of the large volume of major element chemical data available from Tenoumer, these rocks were chosen for studies of the behavior of the lithophile trace elements and the isotopes of strontium. Preliminary results have been reported by Winzer, 1975, and Winzer and Lum, 1976, and these results indicate that the trace element compositions of the melts cannot be explained in the same manner as the major element compositions. Further analyses were made, with the result that at least two explanations of the trace element content were possible, but neither was in any way similar to the explanation for the major element compositions given by Fudali (1974). Detailed petrographic and petrologic analysis of the impact melts themselves had not been done by any of the previous researchers, thus such analyses were undertaken in order to clarify the composition of glasses and melts, and the crystallization history of these melts.

Petrography and petrology

Four polished electron microprobe mounts representative of dikes of the northwest and southwest swarms have been analyzed by SEM/EDS. The two swarms differ from one another texturally, and in the number and size of

xenocrysts and xenoliths present Though not described previously, melts from the two different locations also differ from one another in liquidus phase and crystallization history

The basic texture of all the melts is intersertal with radiating sprays of subhedral pyroxene or olivine in a groundmass of acicular plagioclase, euhedral titanomagnetite and glass (Fig. 1 a-c). Chief differences among the sections and between geographic locations are in grain size (of the crystals from the melt), vesicularity, and number and size of included fragments.

The coarsest grained melt rocks are generally those with the fewest fragments. These also tend to be the rocks which are the least vesicular. The coarse-grained rocks have a random intersertal texture consisting of subhedral low calcium pyroxene, rimmed by high calcium pyroxene (up to 200 μm in length) set in a matrix of lath shaped plagioclase (An_{45}-An_{65}) (up to 500 μm in length) and glass which contains cubes of titanomagnetite (< 10 μm) and droplets of what also appears to be titanomagnetite (generally 2 μm or less) The glass is quite siliceous (up to 70% SiO_2) and contains from 7-9% K_2O + Na_2O (Table 1, Fig. 2). Pyroxenes are variable in composition (Fig 3) and occur in three major textural forms: 1) as discrete euhedral to subhedral grains of relatively constant composition throughout the entire range shown in Fig. 3 when sampled over an entire portion of a thin section, 2) as rimmed subhedral cores and high Ca pyroxene rims; and 3) as subhedral grains with very small inclusions of olivine This last type is very rare.

Plagioclase compositions (Fig. 4) show less of a range from grain to grain, and are unzoned within the range detectable by the EDS system.

Variations in texture can be seen in areas immediately adjacent to larger clasts or xenocrysts in the coarser-grained melts. In areas

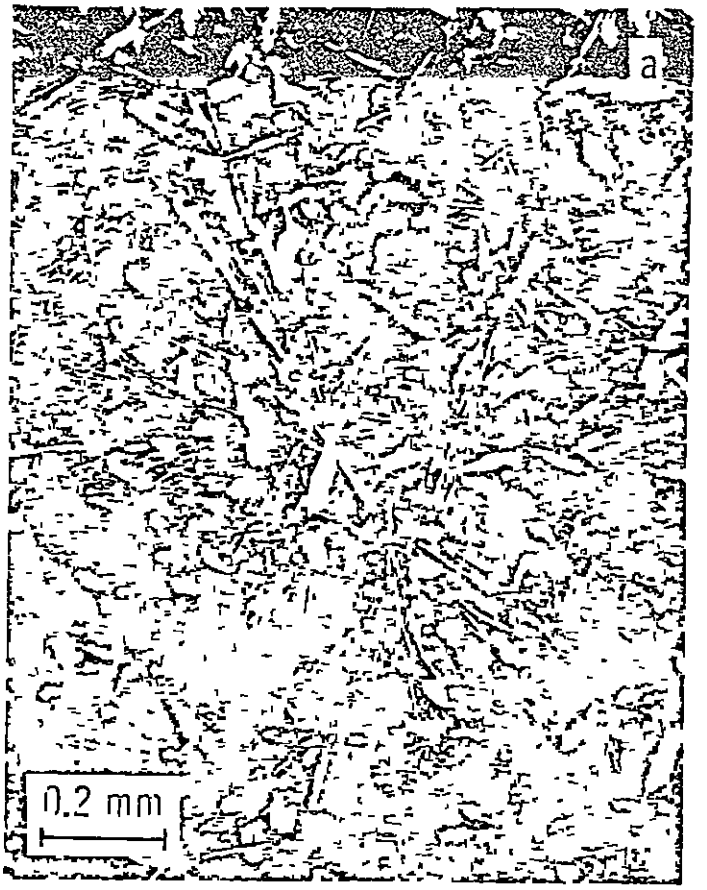

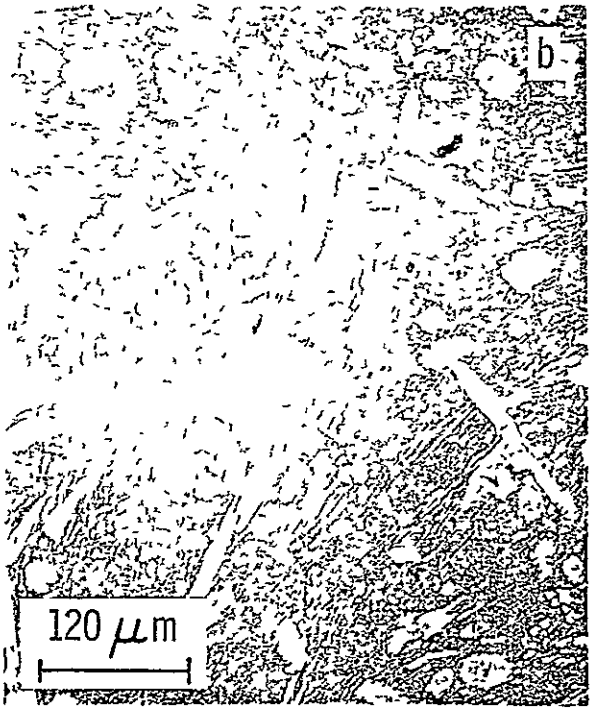

FIGURE 1

ORIGINAL PAGE IS
OF POOR QUALITY

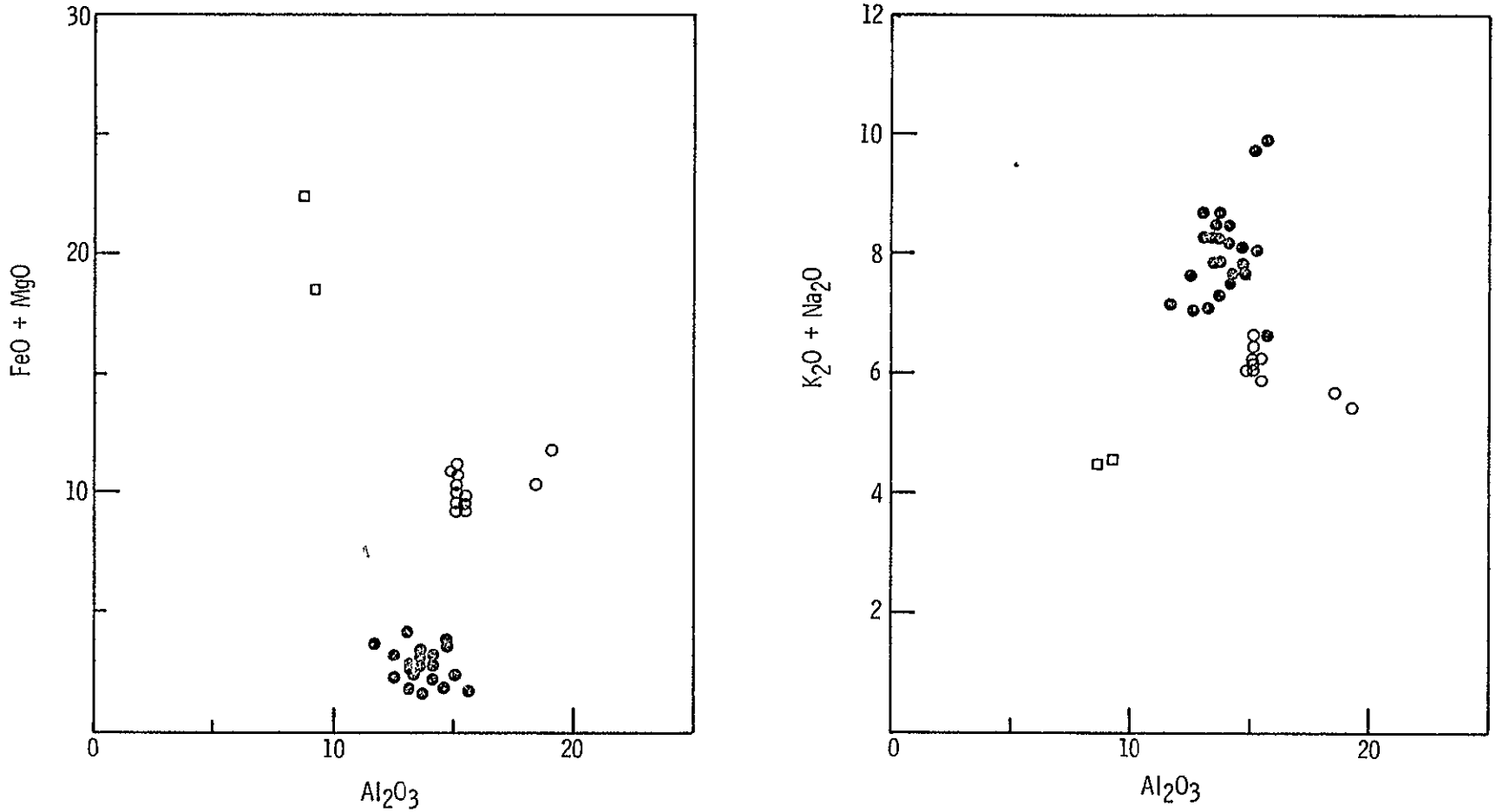

FIGURE 2

FIGURE 3

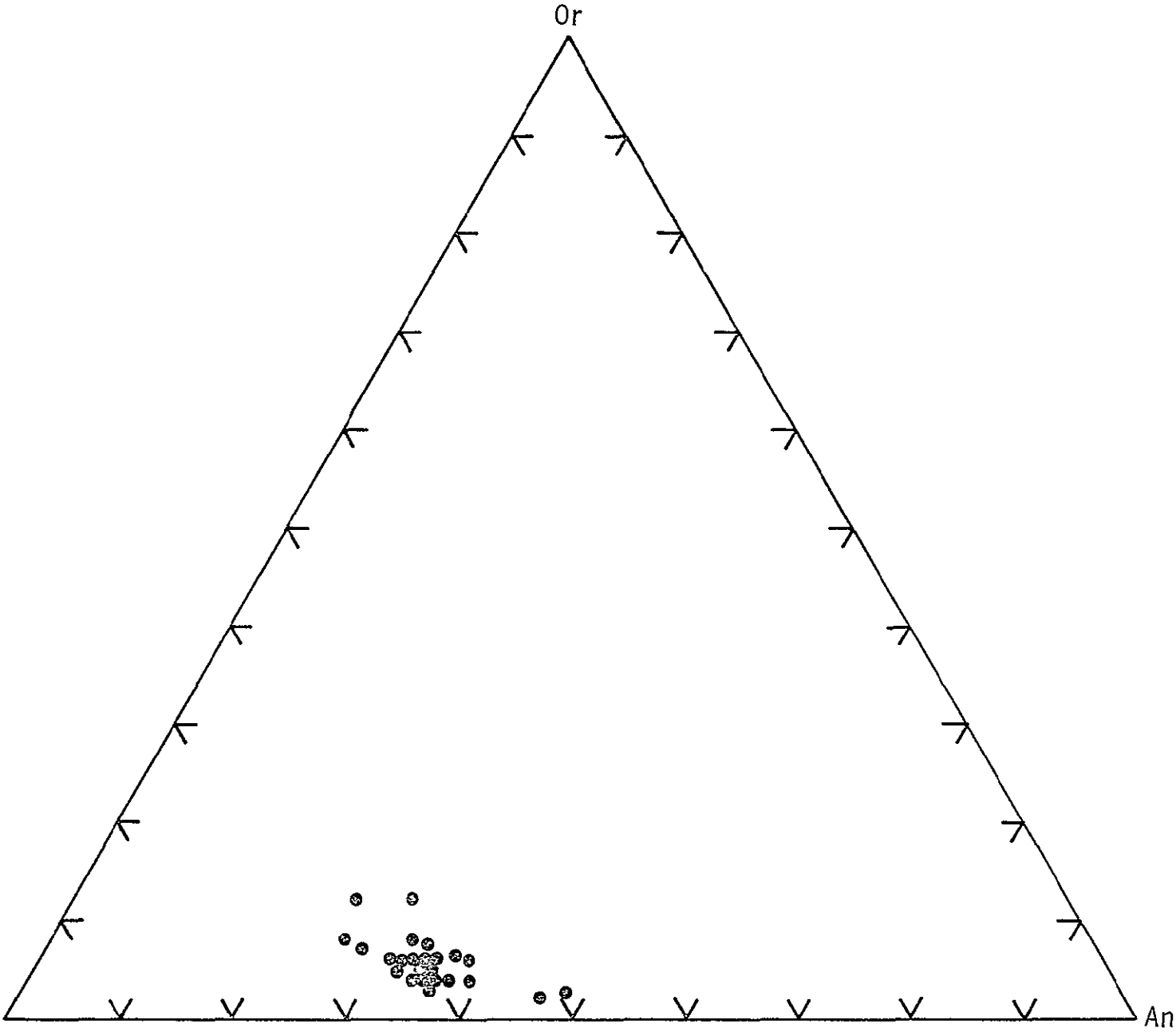

FIGURE 4

immediately adjacent to larger clasts, the melt has developed an irregular vesicularity -- in places, almost an open framework in which the plagioclases have become more acicular in form and the size of the pyroxenes has decreased. Rims on pyroxenes are smaller, and some pyroxenes contain small olivine inclusions (Fig. 5a).

Areas surrounding smaller xenocrysts (usually quartz) are generally different. They are not vesicular, and are marked by a decrease in plagioclase and pyroxene grain size (Fig. 5b). Near the xenocryst a necklace of anhedral pyroxene crystals has formed. Inside this necklace, plagioclase crystals are rare or entirely absent The material inside the necklace is mainly glass containing small subhedral pyroxene crystals.

The finer-grained fragment-laden melts, mainly collected from the southwest dike swarm, exhibit an entirely different crystallization history, although they resemble the coarser-grained rocks texturally. The fine-grained melts are also intersertal, but with small skeletal olivine crystals as the first phase to crystallize (Fig. 6a). These olivines, subhedral to euhedral in shape in the better formed crystals, enclose small, round areas of glass. In the best developed specimens, the glass inclusions resemble a string of beads along the length of the crystal. (Fig 6b). These glasses are of distinctly different composition than the matrix (mesostasis) glass (Table 1). They have a considerably greater compositional range than the mesostasis glasses, and are uniformly higher in FeO + MgO content (Fig. 7) The matrix of the fine-grained melt rocks consists of acicular plagioclase, feathery to irregularly shaped subhedral pyroxene and glass (Fig. 6b and c) Pyroxene compositions, where obtainable, are similar to those in the coarser grained melt

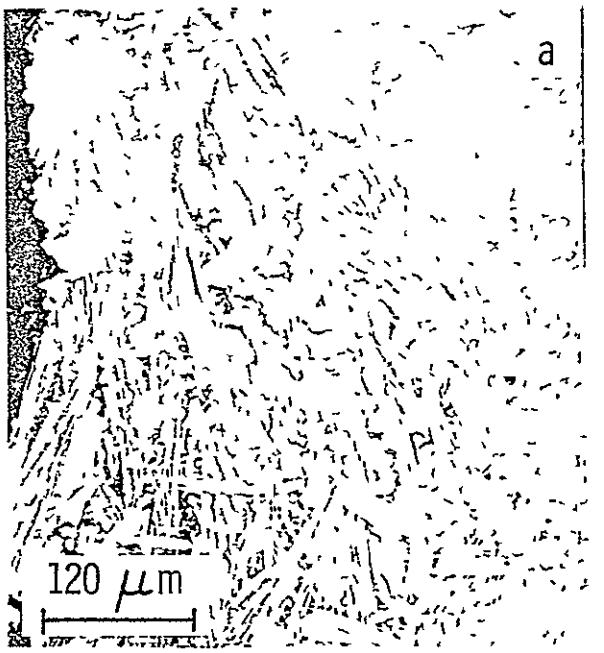

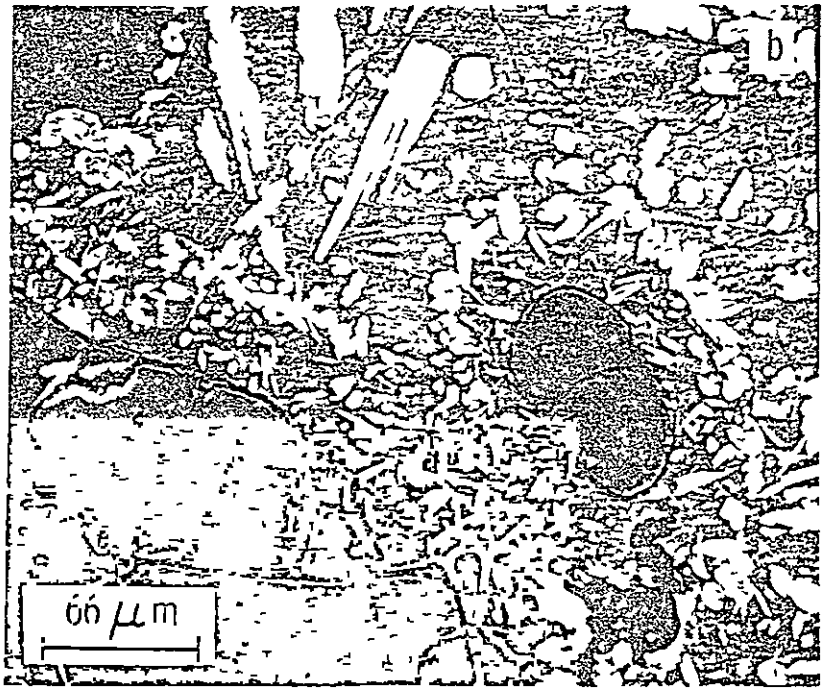

FIGURE 5

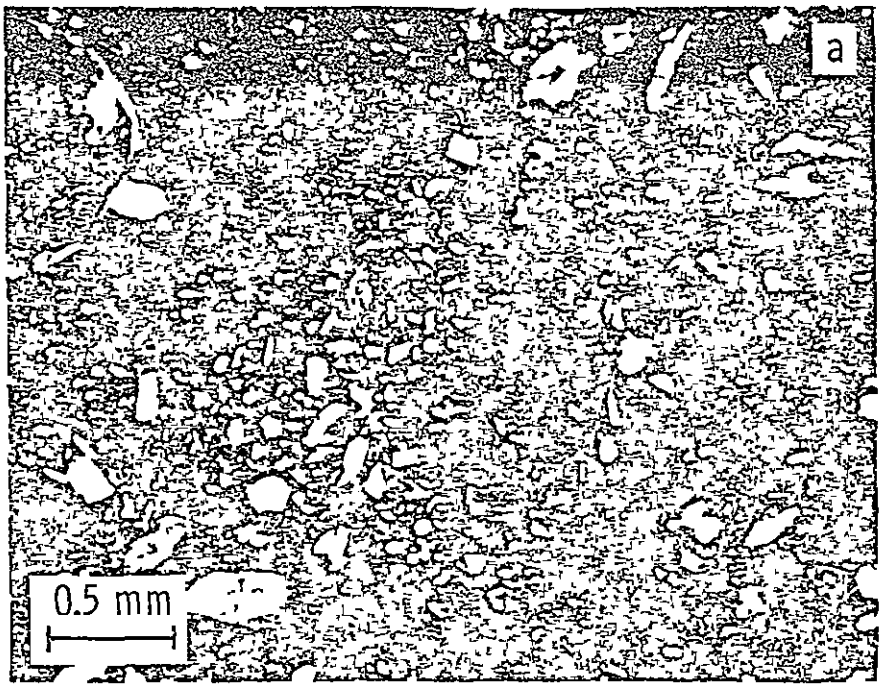

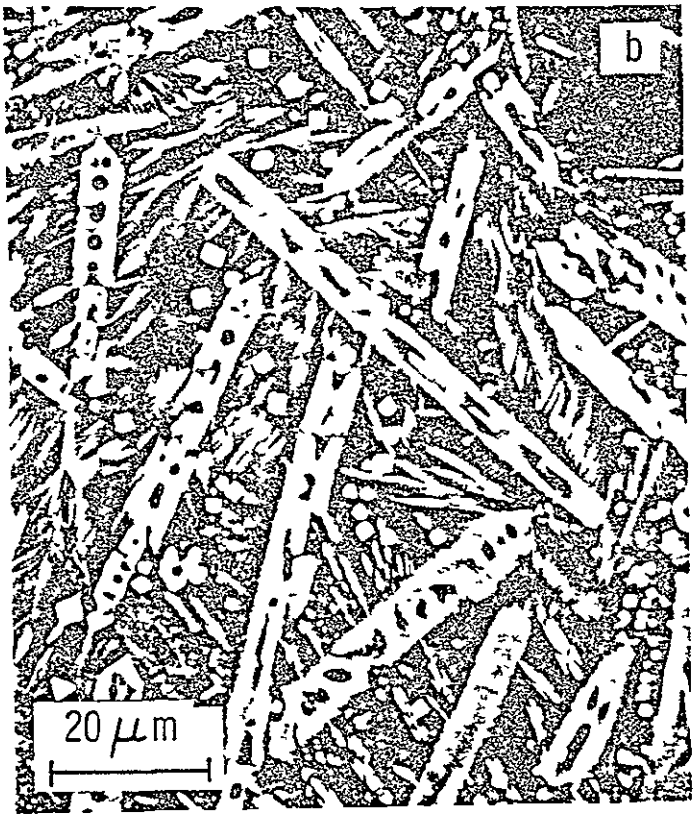

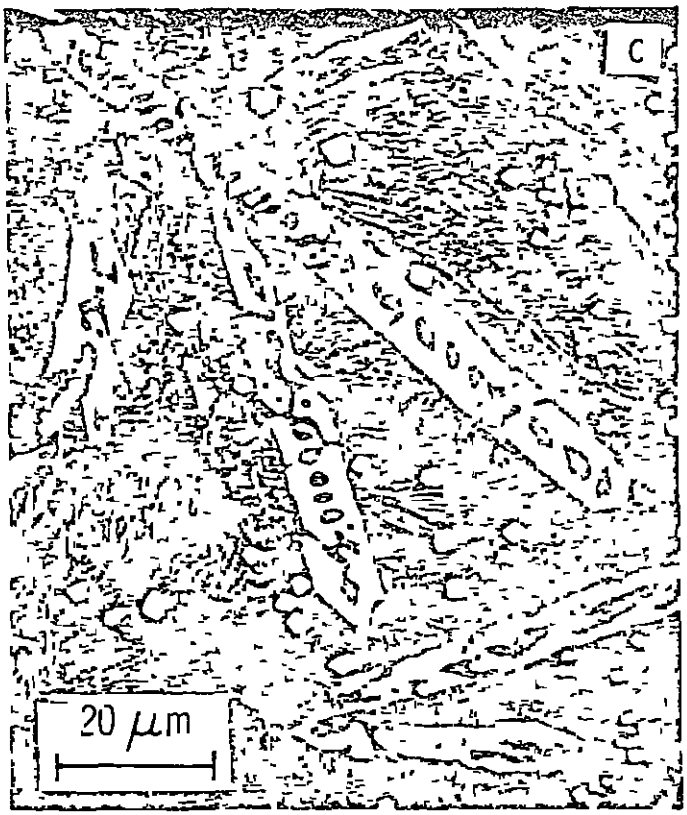

FIGURE 6

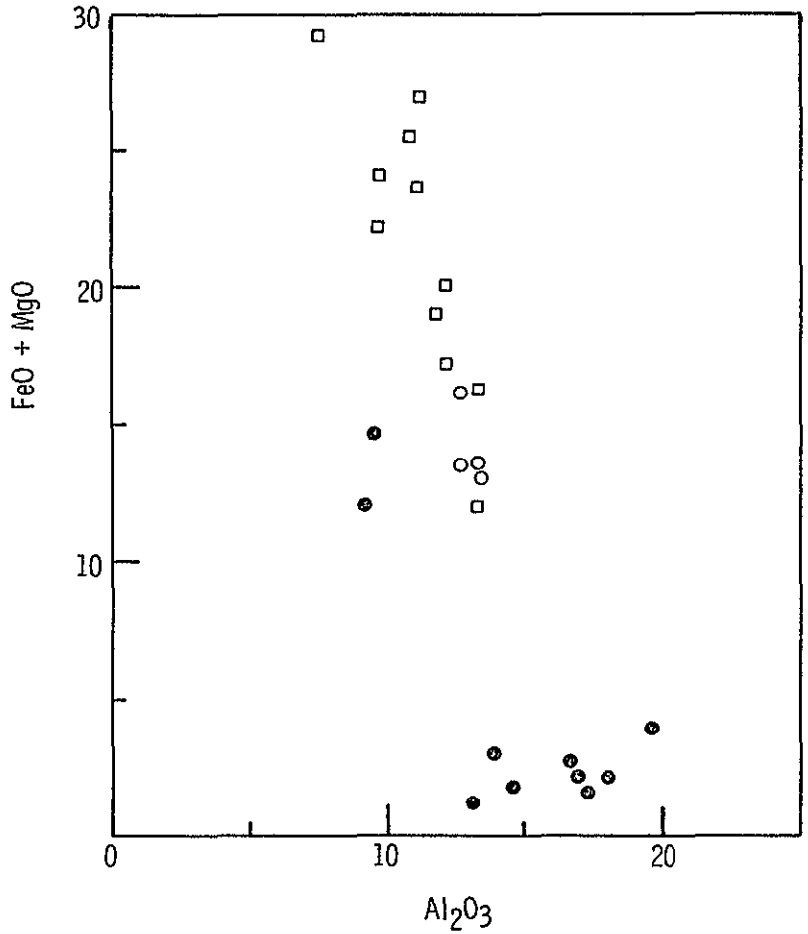

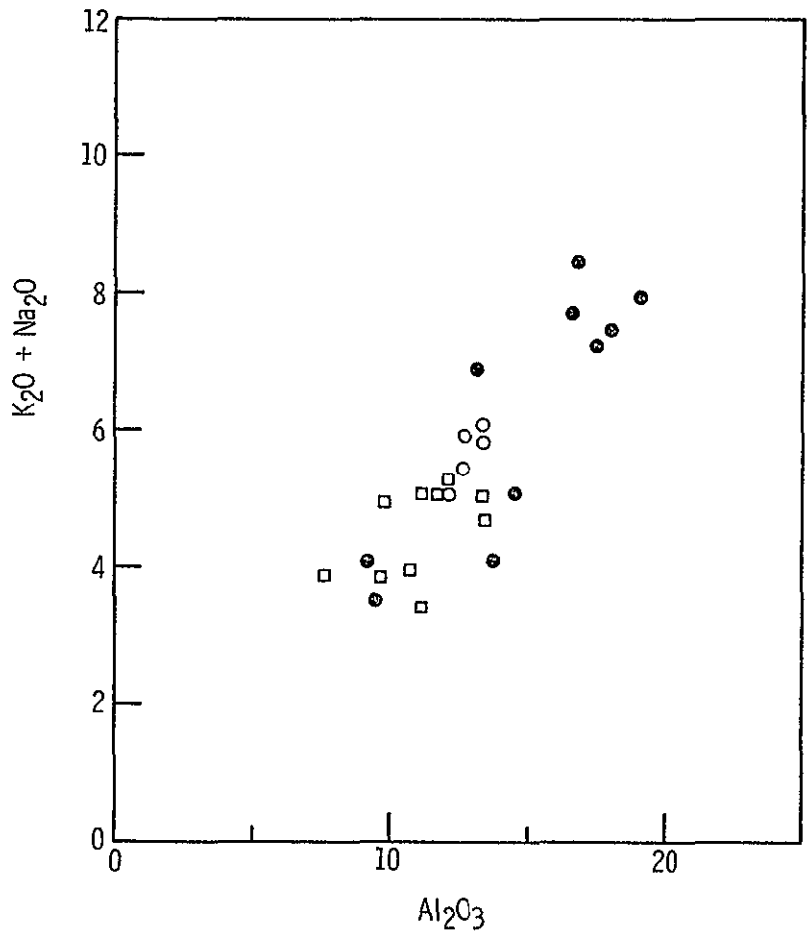

FIGURE 7

rocks (Fig 8), but a few are significantly more calcic. Pyroxene compositions calculated from Niggli normative minerals are less magnesian than pyroxenes which were analyzed, but show the same range of Ca content. Feldspars show a somewhat greater range of An content (Fig 9) than those of the coarser-grained rocks. Normative plagioclases generally calculate in the forbidden area of feldspar compositions, which suggests that if crystallization had continued, potassic feldspars would have crystallized independently of the plagioclase series.

A third, distinctive set of pyroxene compositions can be found in areas immediately adjacent to xenoliths and xenocrysts in coarse and finer-grained melt rocks. These pyroxenes, described earlier as interstitial to fine-grained radiating acicular plagioclases, are more iron-rich than the dominant matrix pyroxenes. Examination of Fig. 3, and comparison with the normative pyroxene compositions calculated from glasses (Fig. 8) indicate that these pyroxenes represent the most iron-rich of all ferromagnesian phases analyzed These pyroxenes are found millimeters or less from normal mesostasis pyroxenes, but the paragenetic sequence which can be deduced from the SEM photographs clearly indicates that they were among the last phases to crystallize (Fig. 10).

Comparisons of glass compositions and mineral analysis indicates that the fine-grained fragment-laden melt rocks tend to be more heterogeneous than the coarser-grained fragment-free melt rocks. All melt rocks tend to be heterogeneous on the microscale. Examples are the pyroxene compositions in the areas surrounding xenocrysts found in the northwest dike swarm rocks, and the mesostasis pyroxenes from the same thin section.

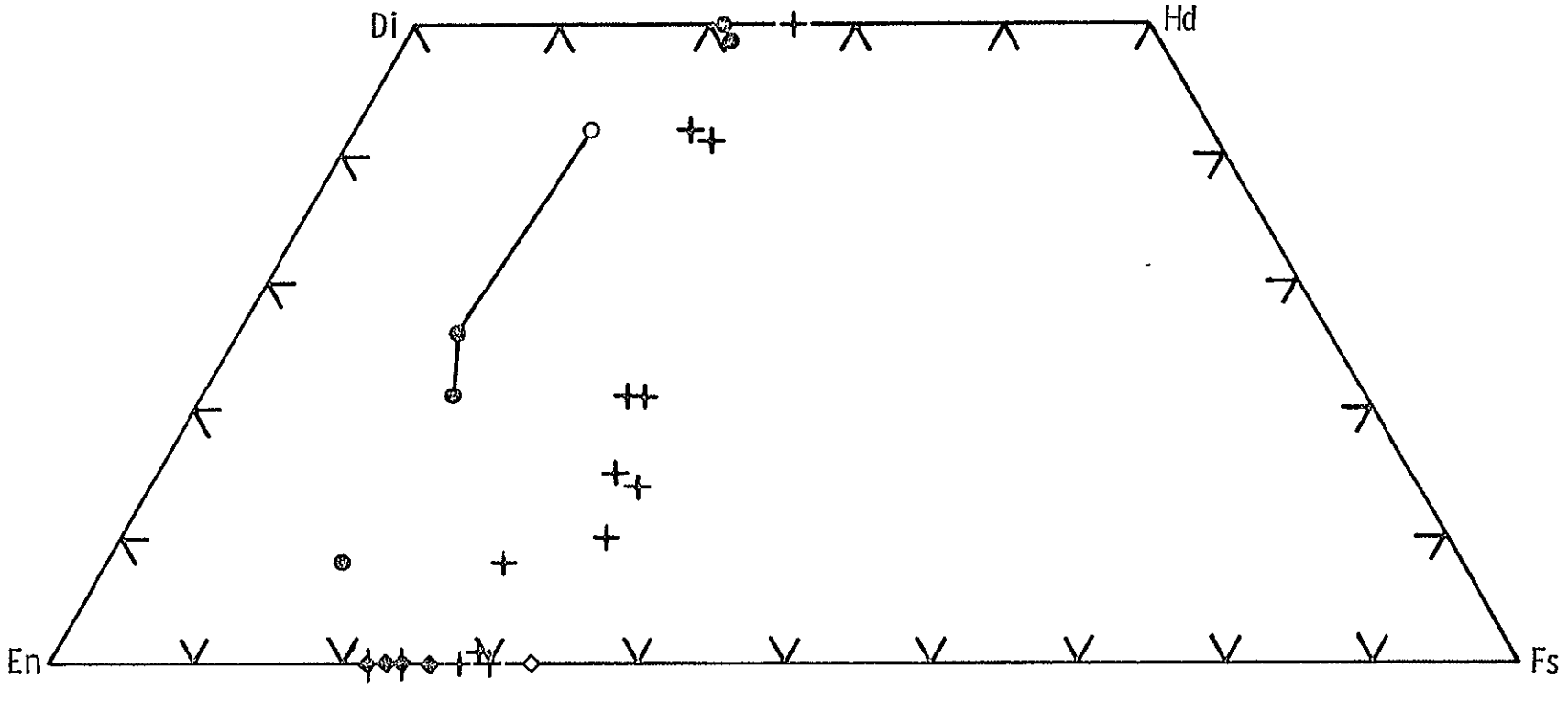

FIGURE 8

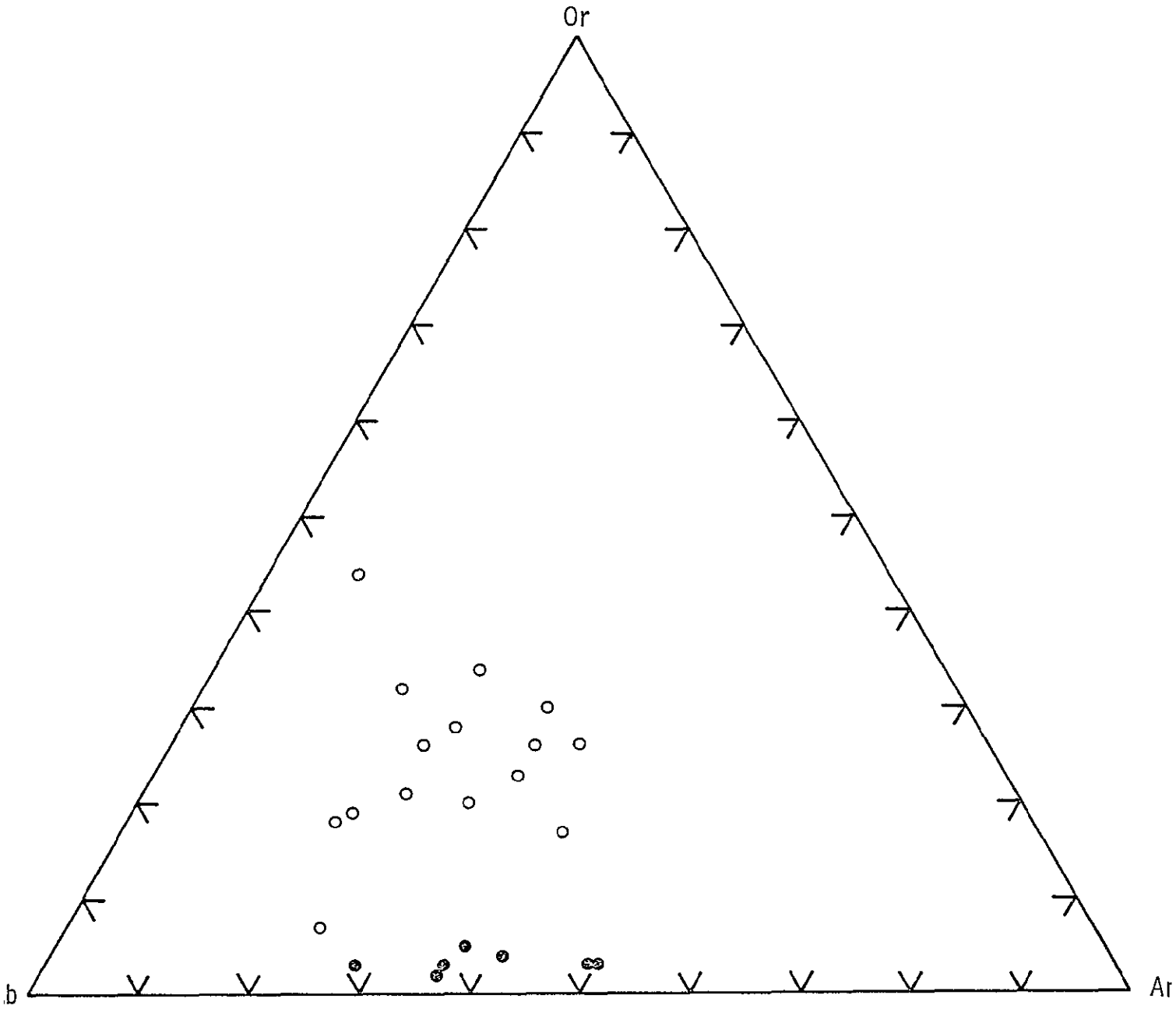

FIGURE 9

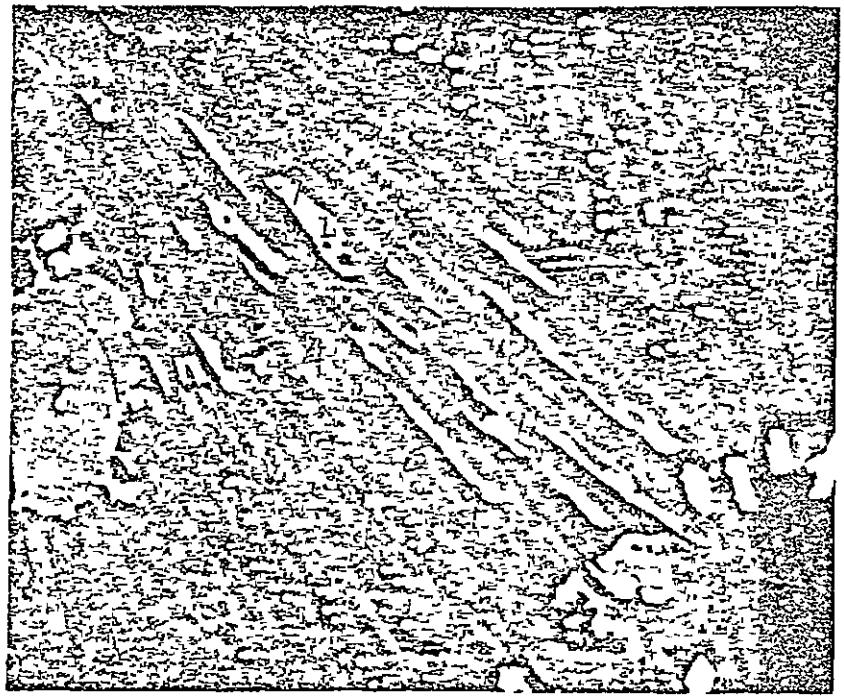

FIGURE 10

Based on detailed examination of the melt rocks, a paragenetic sequence (crystallization history) can be reconstructed. For the fine-grained fragment-laden melts, typified by rocks of the southwest dike swarm, olivine is the first mineral to crystallize. The shape of the olivines found in these rocks most closely resembles the chain and hopper olivines produced at cooling rates of up to 50°C/hour (Donaldson, 1976), but the olivine shapes do not indicate the more rapid cooling rates expected of quenched glasses. Titanomagnetite appears to crystallize simultaneously, forming isolated, well formed cubes scattered throughout. Olivine and magnetite crystallization is followed by crystallization of lath-shaped and acicular plagioclase feldspars. The feldspar morphology is consistent with morphologies of experimentally grown plagioclase feldspars at ΔT of up to 100°C. The exceptions are to be found as radiating acicular grains several hundred microns long but only 5-10 μm across These spherulitic plagioclases are indicative of growth at ΔT above 100°C and possibly above 200°C (Lofgren, 1974). Concurrent with crystallization of fine-grained feldspars is the crystallization of feathery, fine-grained pyroxene crystals. These pyroxenes, which have a dendritic appearance, fill the interstices between olivine crystals, and interfinger with plagioclase crystals. The form of the pyroxene is suggestive of very rapid cooling rates. This is the final phase to crystallize, the remainder is the mesostasis glass, which is filled with small droplets of titanomagnetite

The coarser-grained melt rocks, which are generally free of xenocrysts or xenoliths, crystallize pyroxene first. Morphological and chemical analyses suggest that the first-crystallizing pyroxenes were low Ca pyroxenes with an enstatite content of around 77 mol %. This interpretation is complicated by the

fact that pyroxenes with Wo contents from 10-40% can be found throughout the rock, but the principal composition which forms the cores of the rimmed pyroxenes is ~$Wo_{10}En_{77}Fs_{13}$. Crystallization of low Ca pyroxene was followed by plagioclase, and plagioclase + high Ca pyroxene and titanomagnetite. Pyroxene and plagioclase morphologies are consistent with slower cooling or smaller degrees of undercooling (< 100°C ΔT). Exceptions to this sequence are to be found in regions near clasts or xenocrysts, wherein acicular, radiating plagioclases form, with small, anhedral interstitial pyroxenes of higher Fs content than surrounding pyroxenes. Larger pyroxenes often contain small, anhedral olivine crystals as inclusions. This same paragenesis occurs in one of the coarser grained fragment-laden melts, where lath shaped plagioclase is intimately intergrown with anhedral to subhedral pyroxene. The larger pyroxene grains enclose small, anhedral olivine crystals.

In summary, a paragenetic sequence can be established in the Tenoumer rocks. The fragment-free melts crystallize a low Ca pyroxene and titanomagnetite followed by high Ca pyroxene and plagioclase. In later stages of crystallization, low and high Ca pyroxene, plagioclase and titanomagnetite crystallize together. In the coarser-grained melts which contain xenoliths and xenocrysts, and in areas near larger clasts, olivine has crystallized first, followed by low Ca pyroxene It is likely that olivine has reacted with the melt to form pyroxene, as the olivine always occurs as inclusions in the pyroxene. In the fine-grained fragment-laden melts, olivine and titanomagnetite crystallize first, followed by plagioclase and pyroxene.

Different textural relationships between minerals in the different types of melts indicate dissimilar cooling histories, however, compositional differences

also exist between melts, thus the different crystallization histories and paragenetic sequences are likely a function of both.

Geochemistry

In addition to detailed petrologic studies, selected samples from Tenoumer crater have been analyzed for major, minor and trace elements by a combination of wide-area analysis and isotope dilution mass spectrometry. Wide-area analyses were done using a scanning electron microprobe equipped with an energy-dispersive spectrometer and multi-channel analyzer. The analyses are corrected by the Bence-Albee correction procedure (Bence and Albee, 1968), but are not further corrected at this time. Isotope dilution mass spectrometric analysis for lithophile trace elements follows the method of Schnetzler et al. 1967.

Results of area analyses for NW and SW dike melts are presented in Table 1 These analyses, done by averaging several areas on a single section, are in substantial agreement with the wet chemical analyses of Fudali, 1974. These data were taken with care to avoid including xenocrysts and xenoliths, while those of Fudali are of the bulk rock and thus include xenocrysts and xenoliths. It is somewhat surprising that such agreement is found. The data suggest that the melts do not differ significantly from the composition of their xenocrysts and melt mixtures, and thus support Fudali's contention that the melts result from mixes of granodiorite and amphibolite country rocks.

The trace element geochemistry is not so easily interpreted, however. Lithophile trace element abundances are presented in Table 2 and in Fig. 11. It is immediately obvious from examination of Fig. 11 that not all trace element

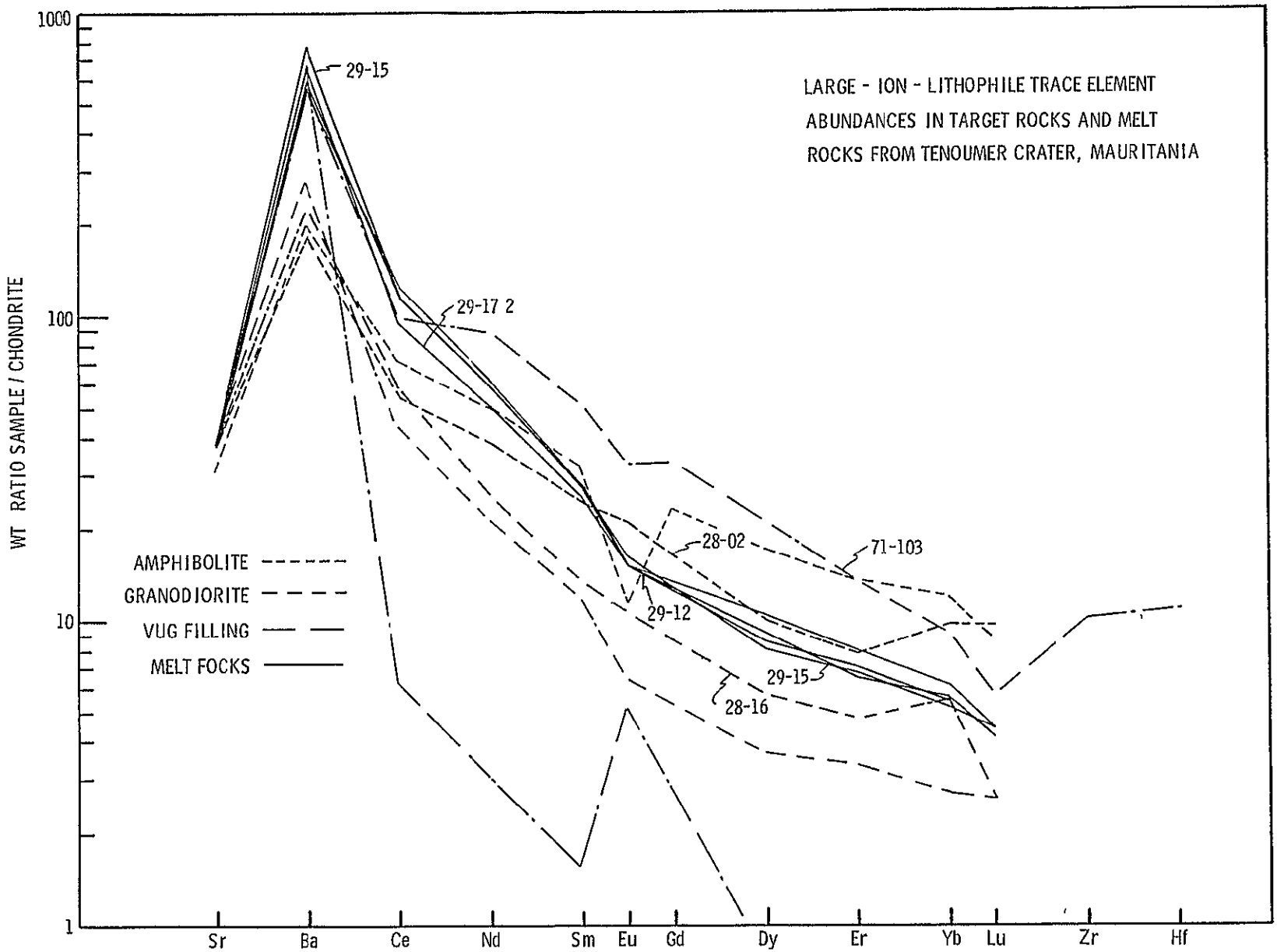

FIGURE 11

TABLE 1

Area Analyses and Mesostasis Glass Analyses*
Tenoumer Crater Melt Rocks
(Wt %)

	Area Analysis** 113019/064		13029/014		Glass Analyses, NW Dike Swarm CL 334	AR4-18-6	AR4-IC-3	CL3-1-2	CL3-1-3	CL3-1-11	CL3-1-12
SiO_2	61 18	2 15	57 69	1 11	69 38	74 53	69 99	75 49	74 62	69 85	70 99
TiO_2	99	12	1 13	09	1 04	1 29	1 13	0 81	0 72	1 10	1 18
Al_2O_3	15 79	1 41	17 91	56	15.94	13 30	15 64	13.08	13 67	15 35	15 67
FeO	6 17	45	8 17	1 03	2 76	2 84	2 76	1 73	1 35	2 32	1 56
MnO	.11	11	12	03	---	---	---	---	0 23	---	0 22
MgO	4 05	52	6 68	89	---	---	0 68	---	0 23	---	---
CaO	5.57	35	6 15	39	1 86	0.92	3 14	0 56	0 66	1 76	0 61
Na_2O	4 15	26	3 78	49	6 97	2 25	3 85	3 06	3 24	7 38	3 86
K_2O	2 04	32	1 88	17	2 10	4 85	2 80	5 33	5 37	2 32	5 99

	CL3-3-4	AR5-3-3	AR5-3-4	AR5-3-12	AR5-3-13	AR5-2-10	AR1-1-3	AR1-2-7	AR1-1-5	AR1-4-1	AR1-4-2
SiO_2	69 38	72 12	71 42	53 38	58 51	71 56	70 77	69 36	72 27	71 05	72 53
TiO_2	1 04	0 80	0 82	6 33	5 78	1 13	1 50	1 42	1 30	1 52	1 28
Al_2O_3	15 94	14 89	15.36	8 54	9.22	13 60	14 78	14 80	14 16	14 10	13 67
FeO	2 76	1 75	1 95	20 90	16 83	3 13	3 56	3 84	2 64	3 36	3 35
MnO	---	---	---	0 28	0.15	0 19	---	---	---	0 26	0 16
MgO	---	0 23	0 43	1 74	1.33	0 27	---	---	---	---	---
CaO	1 86	2 23	2 11	3 64	3.39	2 82	1 79	2 84	1 55	1 36	1 42
Na_2O	6 97	4 02	3 73	2 17	1 98	3 28	5 38	4.53	5 61	5 86	4 89
K_2O	2 10	4 09	4 30	2 37	2 53	4 09	2 34	3 28	2 65	2 61	2 78

*SEM/EDS
**Column 1, average, column 2, 1σ
---Below detection limit for EDS analysis

TABLE 1 (CONTINUED)

	Area AR-1-4-3	AR2-1-7	AR2-1-11	AR2-1-16	AR3-1-4	AR3-1-6	AR3-1-7	AR3-1-8	AR6-2C-1	AR6-2C-3	AR6-2C-5
SiO_2	70 53	73 97	74 27	73 43	73 82	73 37	74 40	74 36	70 00	73 90	75 47
TiO_2	1.51	1 14	0 93	1 00	1 35	1 44	1 51	1 79	0 81	0 98	1 13
Al_2O_3	13 08	13 32	14 34	13 63	13 51	13 43	12 54	11 70	13 54	14 16	12 57
FeO	4 24	2 31	2 20	2 77	2 52	2.58	3 27	3 82	1 80	1 96	2 33
MnO	0 15	---	---	---	0 15	---	---	---	---	---	---
MgO	0 24	0 37	---	---	0 30	---	---	---	0 26	---	---
CaO	1 62	0 79	1 03	0.87	0 74	0 64	1 13	1 09	6 16	1 49	0 88
N_2O	6 12	3 24	2 38	2 82	2 32	3 62	2 17	2 06	2 62	3 07	2 19
K_2O	2 58	5 10	4 81	5 47	5 22	4 86	4 88	5 09	4 04	4 47	5 43

	Glass Analysis, SW Dike Swarm										
	AR1-4-4	AR1-4-5	AR1-4-6	AR1-3-1	(In ol) AR1-3-5	(In ol) AR1-3-7	(In ol) AR1-3-8	AR1-5-1	AR1-5-2	AR1-5-3	(In ol) AR1-5-6
SiO_2	74 20	74 28	58 26	76 27	58 49	60 26	58 43	67 65	68 78	66 79	55 53
TiO_2	1 29	1 23	1 38	1 29	0 70	1 22	0 99	1 43	1 49	1 89	1 25
Al_2O_3	13.79	14.19	9 54	13 23	12 05	13 48	11 81	18 03	17 38	16 97	11 43
FeO	2 98	2 42	9 08	1.11	9.09	7 49	8.66	1 84	1 59	2 22	9 70
MnO	---	---	---	---	0 18	0 24	---	0 23	---	---	---
MgO	---	---	5 76	---	10 78	8 94	10 51	0 37	---	---	14 71
CaO	0 80	0 90	12 31	1 17	2 44	3 34	4 40	2 90	2 82	3 60	2 20
N_2O	2 91	2 91	1 81	3 26	3.01	2 09	3 17	3 85	3 89	4.92	1 91
K_2O	4 14	4 10	1 70	3 60	2 36	2 55	1 86	3 58	3 72	3 55	2 62

TABLE 1 (CONTINUED)

	(in ol) AR1-5-7	(in ol) AR1-5-8	AR1-5-14	AR2-3-4	AR2-3-5	(in ol) AR2-3-9	(in ol) AR2-3-10	(in ol) AR2-3-12	(in ol) AR2-3-14
SiO_2	56 41	55 25	67 44	60 62	59 68	52 91	56 53	55 81	54 86
TiO_2	0 79	1 57	1 60	2 46	1 14	1 14	1 07	1 69	1 12
Al_2O_3	11 16	10 89	16 64	9 31	19 70	11 27	9 91	13 41	7 54
FeO	9 77	10 71	2 06	8 76	3 11	10 63	10 88	7 35	13 11
MnO	---	---	---	---	---	0.36	0 31	---	---
MgO	14 01	14 88	0 71	3 27	0 72	16 37	13.29	4 98	16 19
CaO	2 28	1 85	3 58	11 48	7 69	2 93	1 85	11 54	3 35
Na_2O	2 29	1 86	4 16	2 14	6 78	1 61	2 54	3 17	2 46
K_2O	2 75	2 12	3 62	1 99	1 15	1 81	2 43	1 89	1 37

TABLE 2

Lithophile Trace Element Abundances in Target and Melt Rocks from Tenoumer Crater, Mauritania
(ppm)

	SW Dike 29-12	SW Dike 29-15	SW Dike 29-17 2	NW Dike Ten 71-2C2	Amphibolite 28-02	Amphibolite Ten 70-2	Granodiorite 28-16	Country Rock 113027/372
Li	12 0	14 3	13 9	11 9	10 1	10 1	19 9	
K				17900				
Rb				10 8				
Sr	420	399	407	396	407	357	413	345
Ba	2156	2809	2417	1930	674	837	841	738
Ce	90 0	90 3	74 5	98 5	43 1	44 4	45 1	57 2
Nd	33 7	34 2	29 7	36 2	22 5	22 6	14 9	29 8
Sm	5.14	5 07	4 75	5 18	4 55	4 53	2 48	6 44
Eu	1 07	1 16	1 08	1 10	1 50	1 48	0 744	0 825
Dy	2 68	2.45	3 70	3 25	3 04	3 34	---	5 33
Er	1 28	1 21	1 19	---	1 42	1 44	0 866	2 52
Yb	1 03	0 978	1 05	1 18	1 83	1 09	1 02	2 29
Lu		0 152	0,142	0 154	0,33	0,149	0 089	0 305
Zr				156		90 1		
Hf						2 56		

TABLE 2 (CONTINUED)

	Granodiorite 113027/367	Granite (Red) TEN 713	Vug Filling TEN 71-102	Run 1 BCR-1	Run 2 BCR-1
La		0.487	27 2	13 4	13 0
K					
Rb					
Sr	316	304	361	339	329
Ba	1040	2520	2070	669	653
Ce	35 1	5 10	77 6	55 3	52 7
Nd	12 6	1 82	51 2	29 3	28 8
Sm	2 14	0 296	9 51	6 61	6.56
Eu	0 467	0 380	2 33	1 97	1 94
Dy	1 12	0 169	6 36	6 32	6 36
Er	0 617	0.109	2.44	3 70	3 65
Yb	0 508	0 132	1 71	3 34	3 38
Lu	0 108	0 069	0 197	0 57	0.495
Zr	99 5	9 34	71 3	190	192
Hf			2 19		6 4

--- Below detection limit

abundances can be explained by simple mixing of the endmember compositions chosen by Fudali (1974). Mixing of amphibolite and granodiorite with higher lithophile trace element abundances can explain the compositions of the melt rocks for Sm through Lu, but the light elements cannot be explained in this manner. The melts themselves are all nearly identical in composition, as expected of melts produced by impact (see Winzer et al. 1975, 1977). This, too, is in contrast to the major element compositions which can be explained by mixing. The problem with explaining melt compositions by mixing of any endmembers so far analyzed can best be illustrated by reference to Figs. 12 and 13. Fig 12, a plot of Nd vs Sm abundances in Tenoumer melts and target rocks, illustrates the tight grouping of the melts, and the position of the melts vis a vis the target rocks The melts appear enriched by a small amount over both granodiorite and amphibolite, but they could be explained by addition of some vug material and an as yet undetermined rock type with a higher Nd/Sm ratio. By contrast, Fig. 13 shows that Eu and Sm can be explained by mixing vug filling material with granodiorite and amphibolite The vug filling is a later deposit, not related to the impact itself. It would appear that the best explanation would be that the trace element abundances have been purturbed by the addition of vug filling, however this explanation is not completely satisfactory, as the melts would have to contain almost 100% vug material to be consistent with Ba and Ce abundances. Fudali (1974) calculated the amount of contaminant, and found it to be generally less than 10%. This is in agreement with our observations We must conclude that another as yet unanalyzed component, probably with rather high lithophile trace element abundances, occurs at Tenoumer.

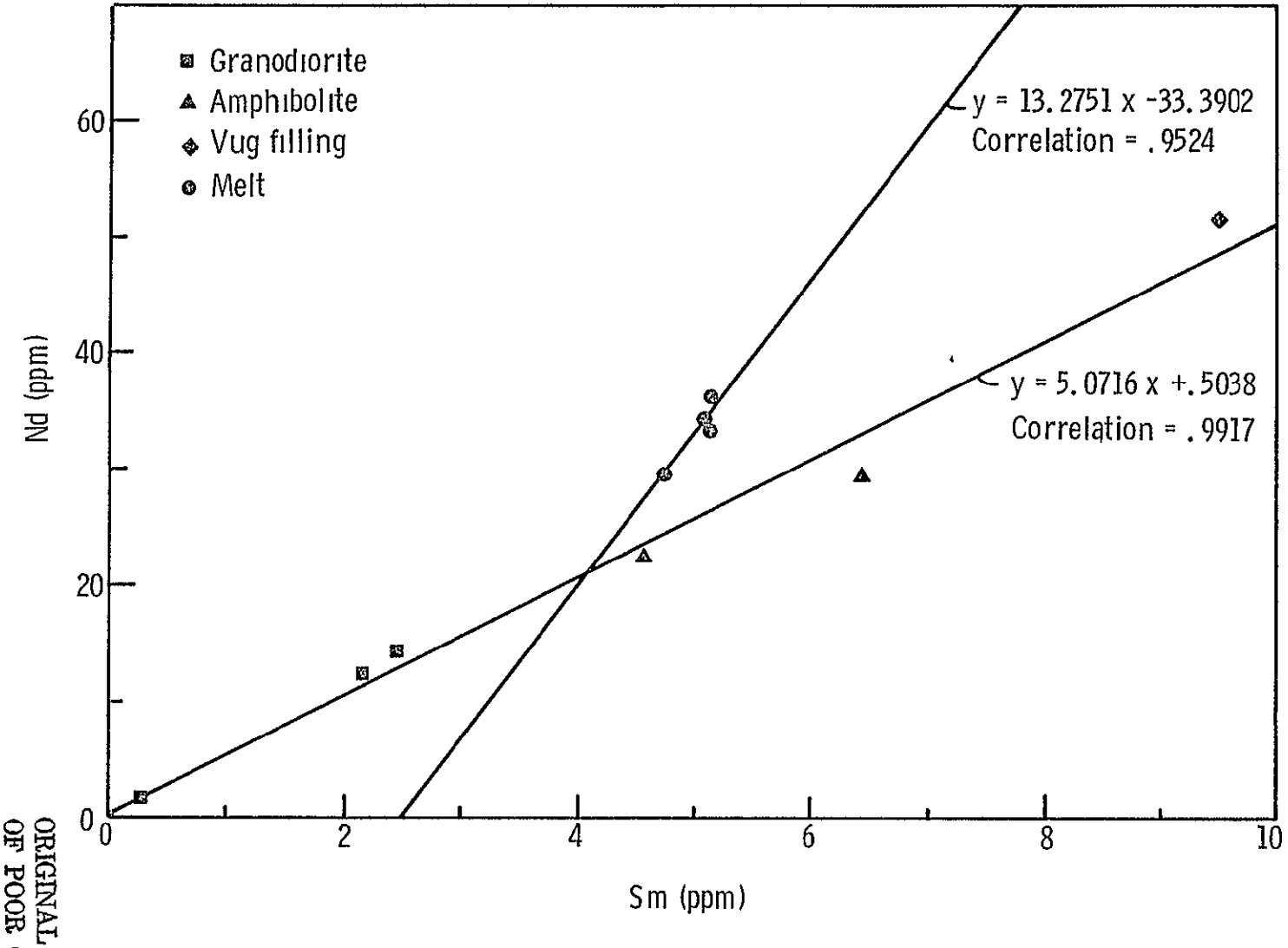

FIGURE 12

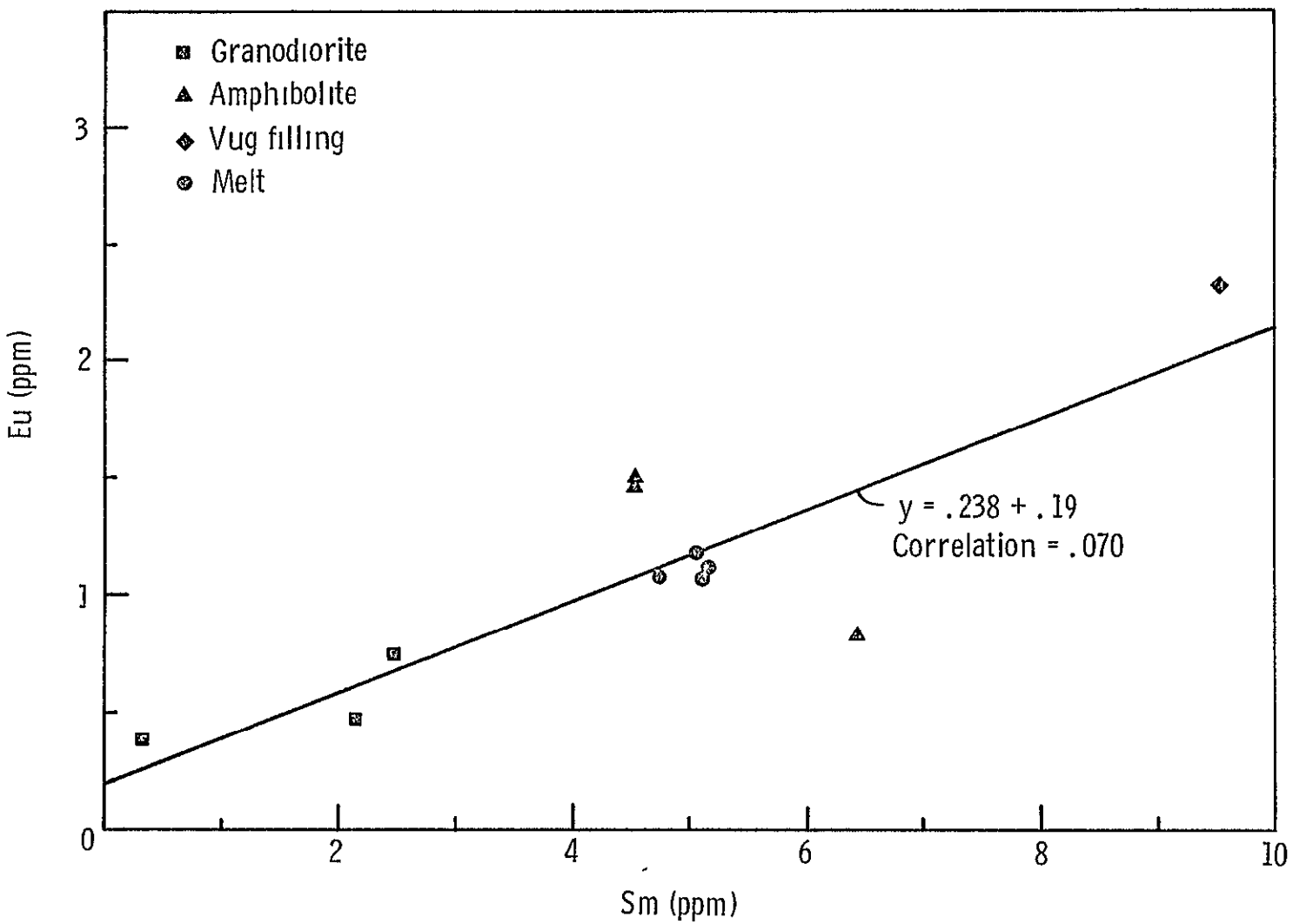
Granodiorite
Amphibolite
Vug filling
Melt
y = .238 + .19
Correlation = .070
Eu (ppm)
Sm (ppm)
0
1
2
3
2
4
6
8
10

FIGURE 13

Summary

The trace element data indicate that the local melting hypothesis put forth by Fudali in 1974 may need some modification If local melting and mixing of amphibolites and grandiorites were solely responsible for the melts, then one would expect these melts to reflect the range of compositions seen in the country rocks. That they do not does not rule out country rock melting and mixing, but suggests another component which would have been involved in all melts. Further collecting and analysis will have to be done to identify this component.

Dellen Lake, Sweden

The Dellen Lake structure, located about 300 km NNW of Stockholm, Sweden, is a poorly defined rounded depression of as much as 10 km in diameter. Associated with this structure is a group of melt rocks, called Dellenites, which have been variously ascribed to volcanic origin (Svenonius, 1895, Redalli 1957 and Magnussen et al. 1963). In a more recent note, Svensson (1968) describes shocked quartz in fragments included in the melt rocks, and concludes from this evidence that Lake Dellen is an impact-produced crater. Three specimens of melt at Dellen have been studied by SEM/EDS and optical microscopy, and samples have been separated and prepared for Rb/Sr and Sr isotopic analysis

Petrography and petrology

The impact melts studied range from fresh, nearly fragment free hyalocrystalline rocks to altered fragment-laden melts Detailed SEM/EDS analyses have been carried out on the fresh, fragment-free melt only. This hyalocrystalline melt contains at most 15% crystalline material.

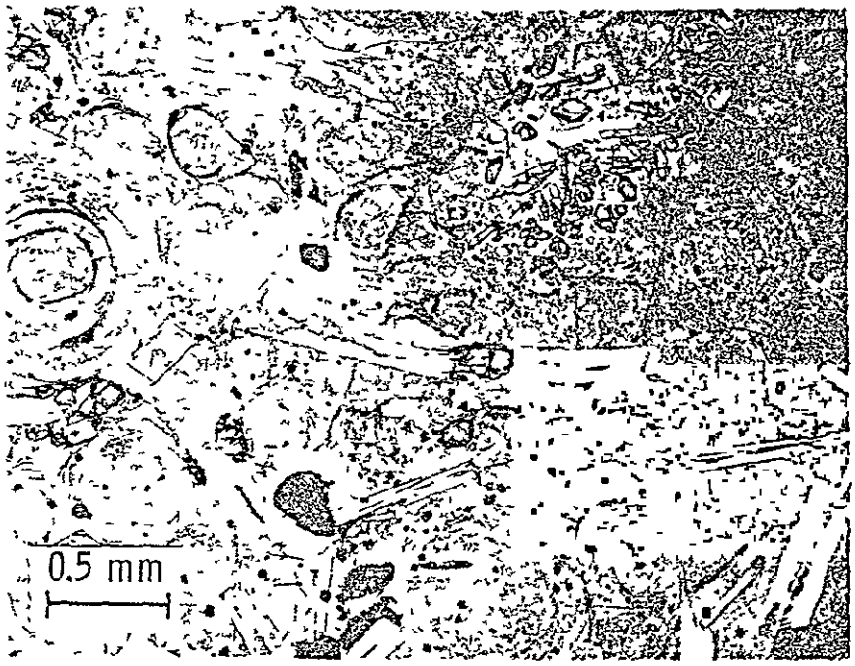

FIGURE 14

TABLE 3

Analyses of Dellen Lake Glasses

	Clear Glass[1] Average	1σ	Brown Glass[2] Average	1σ	Glass enclosed in Px
Wt. %					
SiO_2	75.23	.75	73 63	.52	67.52
TiO_2	43	.14	0.57	.12	0.39
Al_2O_3	13.36	.50	13.62	.28	13.94
FeO	2.45	.33	2.57	.09	5.64
MnO	0.02	.06	0.11	.14	.12
MgO	0.22	.29	0.15	.18	2 87
CaO	0.97	.13	1.22	.19	1.11
Na_2O	2.68	.35	3 89	.31	3.65
K_2O	4 79	.26	4.36	.32	4.75
%					
Ilm	.6		.6		.6
Ab	24.5		35.0		33.0
Or	29.0		25.5		28.0
An	5.0		5.0		5.5
Cor	2.1		1.8		.9
En	.9		.6		8.0
Fs	3.2		3.2		8.2
Qtz	34.7		28.3		15.8

1 Average of 22 analyses

2 Average of 3 analyses

Euhedral to subhedral plagioclases (An_{41} to An_{60}), often zoned ($An_{60} \rightarrow An_{50}$) occur in a random pattern throughout the slide. Plagioclase crystals occasionally show skeletal outlines, swallowtail terminations, or a hopper texture with blebs of enclosed glass along the length of the crystal (Fig. 14). Smaller, equant subhedral orthopyroxene crystals are also scattered throughout the melt. Both pyroxene and plagioclase cluster in subradiating sprays, in addition to their occurrence as isolated crystals. Orthopyroxenes range in composition from Wo_2En_{62} to Wo_2En_{47}. Zoned pyroxene crystals, with cores $Wo_2En_{62}Fs_{36}$ and rims $Wo_{2-3}En_{47}Fs_{50}$ occur throughout the rock. Very small titanomagnetite cubes occur scattered throughout the entire slide. The remainder of the slide is composed of a siliceous glass with a relatively tight compositional range. Table 3 presents average glass compositions for the three major glass types present in the section. Clear glass (transparent or with a slightly reddish color when viewed in transmitted plane light) forms the bulk of this sample. The normative composition of the glass (Niggli norm), is 58 5% feldspar ($An_9Ab_{42}Or_{49}$), 4.1% pyroxene ($En_{22}Fs_{78}$), and 34 7% quartz. The glass is corundum normative The brown glasses, which appear to have partially devitrified, are higher in normative feldspar, but otherwise very similar to the clear glass. Several of the more skeletal pyroxenes enclose glass with a significantly different composition than the surrounding glass. This third type contains 66.5% normative feldspar ($An_8Ab_{50}Or_{42}$), 16.2% pyroxene ($En_{49}Fs_{51}$), and 15.8% quartz. It is also corundum normative.

Discussion

Mineral and glass analyses and textural relationships among these phases indicate a crystallization history and paragenetic sequence for the fragment-free

Dellen melts. All three mineral phases present appear to have crystallized simultaneously. If equilibrium crystallization has occurred from the melt, the normative mineral compositions (in molecular proportions) should nearly equal the actual compositions of the minerals in the rock This is clearly not the case for the bulk glasses; however, the pyroxene compositions overlap those expected from crystallization of the glasses internal to the pyroxene. The feldspar compositions calculated from either glass are not at all like the plagioclases actually crystallized. One would expect, from the normative calculations, that alkali feldspar would be the liquidus phase. Using the normative compositions and the textural relationships between the minerals, a reasonable scenario can be produced. The hot melt probably initially crystallized plagioclase feldspar, depleting the melt in Ca. Crystallization of orthopyroxene followed fairly soon after crystallization of plagioclase, and probably from a melt similar in composition to the enclosed glass Pyroxene crystallization further depleted the melt in FeO and MgO The melt was then very rapidly quenched, so that no further crystallization took place. The composition of the final melt is that of the clear glass. The composition of orthopyroxene and plagioclase from a melt of this composition is unusual. These phases suggest that the melt may have been at very high temperatures, and this would be expected of impact melts.

ZHAMANSHIN STRUCTURE, USSR

The Zhamanshin crater, located near the Irgiz river about 200 km north of the Aral Sea in Kazakhstan, S.S.R., is a small (~10 km) structure which differs from Tenoumer and Dellen in two important aspects. First, it is the only crater of the three in which there is an inner depression surrounded by an

outer ring. Second, the crater has associated with it a number of tektites, making it one of three craters which can or may be directly involved in tektite formation. (Bosumtwi and Ries are the other two). The tektites, called Irghizites, and the shocked and melted rocks of the crater itself are the subject of a study by a consortium of scientists including DeGasperis, Ehmann, Florensky, Fredriksson, Philpotts, O'Keefe, Sclar, Short, and Winzer. The purpose of this study is to relate chemistry, isotopes, petrology, magnetics, age and shock effects of target and melt rock to the Irghizites.

During the past 3 months, samples of Irghizites, melt rocks and shocked target rocks have been received and examined optically. Six samples were chosen for initial studies of lithophile trace element abundances and Rb, Sr, and Sr isotopes. These samples included three Irghizites, one Zhamanshinite (an impact melt) and two target rocks, a cherty limestone and a quartzofeldspathic gneiss. Physical preparation and chemical separation of Sr and Rb have been completed. Mass spectrometry is being done at present. Two papers are to be presented at the 1977 annual meeting of the Meteoritical Society (See Attachment B).

PETROLOGY AND PETROGRAPHY OF LUNAR HIGHLANDS BRECCIAS

Work in the past contract year has concentrated on consortium breccia 61175 and on 15255, a glass-coated fragment-laden melt from the Apollo 15 landing site. This work was undertaken as part of a cross-comparative study of lunar highlands breccias undertaken as part of the study "A study of major and trace elemental and isotopic abundances, mineralogy and petrology, solar wind radiation effects and magnetic properties in returned lunar samples", headed by D. F. Nava of the Goddard Space Flight center.

61175

Apollo 16 sample 61175 is a light matrix polymict breccia designated for consortium study by LSAPT. It has been the subject of a study by a number of scientists for the past year Results of petrographic and petrologic studies and of major and trace element determinations are presented in Attachment B. and in Winzer and Meyerhoff, 1977.

During this contract year studies were begun in conjunction with Dr O.A. Schaeffer, SUNY Stony Brook, to ascertain Ar/Ar and K/Ar ages using laser fusion of selected minerals in clasts which have been described in detail by optical and SEM microscopy and electron microprobe.

15255

15255 is a fragment-laden melt partly enclosed by a vesicular glass rind. Study of this breccia was undertaken as a precourser to possible consortium study Results of this study are presented in Nava et al 1977.

Discussion

15255 and 61175 are very different in provenance, and are indicative of rather different pre and post impact histories. 61175 was not lithified at high temperature, as indicated by the small amount of glass in the matrix, and lack of sintering of the matrix. The clast population in 61175 is diverse and varied on textural grounds, but detailed studies indicate that, with the exception of granulites and hornfelses, the clasts represent impact melts with differing nucleation or cooling histories The only primary igneous rocks present appear to be anorthosites, which have been moderately shocked.

15255, by contrast, is indicative of higher temperatures of formation, as evidenced by larger amounts of matrix glass, and textures indicative of rapid quenching or crystallization from the melt. The clast suite is not nearly so diversified as that of 61175, and few clasts of any size remain in 15255. Those clasts that do remain are suggestive of either gabbroic rocks or mare basalts. The overall composition of 15255 is higher in Fe and Mg and lower in Al than the 61175 breccia. The vesicular glass rind found on 15255, and several other Apollo 15 breccias, is absent from 61175.

When compared to terrestrial impactites, the origin of 61175 and 15255 can perhaps be constrained somewhat. 15255 can be compared to suevite-like breccias of which the type locality is the Ries Crater in Germany. These breccias contain glass veins, schlieren, and fragments of minerals and lithic clasts. They are most commonly found as ejecta, glass bombs, or irregular blocks outside of the crater itself. Suevite breccias appear to grade into glass-poor breccias which are mainly collections of lithic clasts held together by finely comminuted rock powder and small amounts of glass. This variety of breccia is also found as ejecta, but may also be found within the crater itself. The glass-poor fragmental breccias are analogous to 61175. This type of breccia generally contains the most diverse of the clast suites, and many of the fragments and lithic clasts show evidence of shock.

On comparison with the lunar breccias studied, one conclusion can be reached based on petrography and petrology. This conclusion is that neither 15255 nor 61175 are parts of large melt sheets like those found at Manicouagan (Floran et al in prep) or Mistastin (Grieve et al 1974, they are also different from the Apollo 17 breccia boulders which may belong to a single melt sheet (Winzer et al 1977).

These breccias are more likely to be ejecta from lunar craters, and have undergone different formational histories. The differences in texture, reflecting differences in temperature and shock pressure, are likely to reflect derivation from different parts of the crater.

References

Bence, A. E. and A. L. Albee (1968) Empirical correction factors for electron microanalysis of silicates and oxides. J. Geol. 76, 382-403.

Donaldson, C.H. (1976). An experimental investigation of olivine morphology. Contrib. Mineral Petrology 57, 187-213.

Floran, R.J., R.A.F. Grieve, W.C. Phinney, J.L. Warner, C.H. Simonds and D P. Blanchard. Manicouagan impact melt, Quebec. Part I: Stratigraphy, petrology and chemistry. in prep.

Florensky, P.V. (1975) The Zhamanshin meteorite crater (the northern near-aral) and its tektites and impactites Geol. Ser. 10, 73-86.

French B.M., J.B. Hartung, N.M. Short and R.S. Dietz (1970) Tenoumer Crater, Mauritania; Age and petrologic evidence for origin by meteorite impact. Jour. Geophys. Res. 75, 4396-4406.

Fudali, R F. (1974) Genesis of the melt rocks at Tenoumer Crater, Mauritania. Jour. Geophys. Res. 79, 2115-2121.

Grieve, R.A.F., A.G. Plant and M.R. Dence (1974) Lunar impact melts and terrestrial analogues: Their characteristics, formation and implications for lunar crustal evolution. Proc. Lunar Sci. Conf. Fifth p. 261-273.

Lofgren, G. (1974) An experimental study of plagioclase crystal morphology: Isothermal crystallization. Am. Jour. Sci. 274 p. 243-273.

Magnussen, N.H., G. Lundqvist and G Regnell (1965) Severiges Geologi 4th ed. Stockholm.

Monod, Th. and C. Pomerol (1966) La cretère de Tenoumer (Mauritanie) et ses laves. Bull. Geol. Soc. France Ser. 7, 8 165-172.

Nava, D.F., S.R. Winzer, D.J. Lindstrom, M. Meyerhoff, R.K.L. Lum, P.J. Schuhmann, M.M. Lindstrom and J.A. Philpotts. (1977) Rind glass and breccia: A study of lunar sample 15255. Lunar Sci. VIII, 720-722.

Redalli, L.L. 1957: A petrological investigation of Lake Norra Dellen by means of frog-man equipment Sveriges Geologiska Undersökning Ser. C No. 548.

Richard-Molard, J. (1948) Le cratère d'explosion de Tenoumer et l'existance probable d'une grande fracture rectelıgne au Sahara occidentale. C.R. Acad. Sci. Paris 227, 213-214.

Schnetzler, C.C., H.H. Thomas and J.A. Philpotts (1967) Determination of rare-earth elements in rocks and minerals by mass-spectrometric stable isotope dilution technique. Anal. Chem. 39, 1888-1890.

Svenonius, F. in Blomberg, A. (1895) Praktiskt geologiska undersökningar inom Gefleborgs län. Sveriges Geologiska Undersökning Ser C. No. 152, 54-59.

Svensson, N. B. (1968) The Dellen Lakes, a probable meteorite impact in central Sweden. Geol. Fören Stockholm Förh 90, 309-316.

Winzer, S.R. (1975) Does impact produce chemical fractionation? (abs.) EOS Trans. A.G.U. 56, 389-390.

Winzer, S.R. and R.K.L. Lum (1976) The relationship between target and melt rocks in terrestrial craters: Implications for the origin of Lunar breccia matrices. Meteoritics 10, 506-507.

Winzer, S.R., D.F. Nava, S. Schuhmann, R.K.L. Lum and J.A. Philpotts (1975) Origin of the Station 7 boulder: A note. Proc. Lunar Sci. Conf. 6th, 707-710.

Winzer, S.R., D.F. Nava, P.J. Schuhmann, R.K.L. Lum, S. Schuhmann, M.M. Lindstrom, D.J. Lindstrom and J.A. Philpotts (1977) The Apollo 17 "melt sheet": Chemistry, age and Rb/Sr systematics. Earth and Planet. Sci. Lett. 33, 389-400.

Winzer, S.R. and M. Meyerhoff (1977) Petrography and petrology of clasts from consortium breccia 61175. Lunar Sci. VIII, 1017-1019.

Figure Captions

Fig. 1 Optical and scanning electron photomicrographs of melts from Tenoumer Crater, Mauritania.

a) Optical photomicrograph of coarse-grained fragment-free melt, N. W Dike Swarm. Subradiating laths are plagioclase, equant grains are pyroxene

b) SEM photomicrograph, coarse-grained fragment-free melt. Light crystals are pyroxene, darker cores are Ca poor, light rims are Ca rich. Small cubes of titanomagnetite are in glass in between plagioclase laths.

c) Optical photomicrograph of fine-grained fragment-laden melt. Small subhedral grains are olivine, with glass inclusions, feathery crystals are pyroxene. Laths and radiating acicular crystals are plagioclase.

d) SEM photomicrograph of fine-grained fragment-laden melt Light colored, subhedral hopper-shaped and chain olivines enclose glass. Feathery crystals in the mesostasis are pyroxene, droplets and cubes are titanomagnetite.

Fig. 2 a) Al_2O_3 vs FeO + MgO for glasses from coarse-grained fragment-free rocks from the NW Dike Swarm. ⊗ Mesostasis O Area analysis □ included in pyroxene.

b) Al_2O_3 vs K_2O + Na_2O plot for glasses from coarse-grained fragment-free rocks from the NW Dike Swarm. ⊗ Mesostasis O Area analysis □ included in pyroxene.

Fig. 3 Pyroxene compositions from coarse-grained fragment-free rocks from the NW Dike Swarm, Tenoumer Crater ⊘ core ○ rim ◇ olivine ▣ Pyroxene from reaction rims around included xenolith.

Fig. 4 Plagioclase compositions from fragment-free melts, NW Dike Swarm

Fig. 5 a) SEM photomicrograph of vesicular area near large included xenolith, Tenoumer Crater, NW Dike Swarm.

b) SEM photomicrograph or "necklace" texture surrounding a quartz xenocryst, intermediate grain size. Ring is anhedral pyroxene. Acicular plagioclase occurs outside the pyroxene ring and is absent inside it.

Fig. 6 a) Optical photomicrograph of the general texture of fine-grained fragment-laden melt, Tenoumer Crater, SW Dike Swarm.

b) SEM photomicrograph, fine-grained olivine with glass inclusions.

c) SEM photomicrograph of mesostasis area in fine-grained fragment-laden melt. Droplets are titanomagnetite.

Fig. 7 a) Al_2O_3 vs FeO + MgO plot of glass compositions from fine-grained melts, SW Dike Swarm. Symbols as in Fig. 2.

b) Al_2O_3 vs K_2O + Na_2O plot of glass compositions from fine-grained melts, SW Dike Swarm. Symbols as in Fig. 2.

Fig. 8 Pyroxene and olivine compositions from fine-grained fragment-laden melts, SW Dike Swarm ⊘ core ○ rim ◈ olivine and + pyroxene compositions calculated from Niggli norms of glasses from the SW Dike Swarm.

Fig. 9 Plagioclase compositions from fine-grained fragment-laden melt, SW Dike Swarm. ● plagioclase ○ normative feldspar compositions calculated from glasses in SW Dike Swarm melt rocks.

Fig. 10 SEM photomicrograph of area near included xenocryst Tenoumer Crater Fine-grained, acicular light colored mineral is Fe-rich pyroxene. Darker Acicular mineral is plagioclase. Larger, equant minerals are more magnesian pyroxene.

Fig. 11 Lithophile trace element abundances in melt and target rocks from Tenoumer Crater.

Fig. 12 Plot of Nd against Sm for target and melt rocks from Tenoumer Crater.

Fig. 13 Plot of Eu against Sm for target and melt rocks from Tenmouer Crater.

Fig. 14 Optical photomicrograph showing general texture of melts from Lake Dellen, Sweden.

ATTACHMENT A

THE ZHAMANSHIN STRUCTURE: GEOLOGY AND PETROGRAPHY

P. V. Florensky[1], N. Short[2], S. R. Winzer[3] and K. Fredriksson[4].

1) Geological Institute of the Academy of Sciences, Moscow; 2) Goddard Space Flight Center; 3) Martin Marietta Laboratories; 4) Smithsonian Institution.

The Zhamanshin structure, near the Irgiz River 200 km north of the Aral Sea in Kazakhstan, S.S.R., is a concentric disturbance with a 5 km-wide, loess-filled inner depression and a 10 km-diameter outer ring Regional bedrock consists of ~150 m of clays, sandstones, marls, and limestones from Cretaceous to Oligocene in age overlying Paleozoic schists, volcanic series, and carbonates. Fragments and blocks, mainly from the Paleozoic-Mesozoic sequence, comprise an allogenic breccia in variably thick deposits emplaced along hillslopes outside the inner ring. Although shatter cones are absent, the presence in the breccia of fused rock and quartzose rocks containing coesite, thetomorphic minerals and quartz showing planar features led P. V. Florensky and others to postulate in 1969 that the crater was formed by meteorite impact. K/Ar age dating suggests that the event occurred either less than 1 my ago or between 4.8 and 8.1 my. Associated with the crater are dense black glasses (Irghizites) having many chemical characteristics of the Australasian tektites.

Petrographic examination shows several stages in the fusion of bedrock, including transitional decomposition of pyroxene, variable vesiculation, total fusion and degrees of crystallization. One sample, apparently from a quartz vein, is dominantly lechtelierite. Quartz planar features in a chert and an orthoquartzite are atypical in frequency, appearance and orientation relative to most impactites; but planar features in quartz within a carbonate breccia are similar to planar features in Canadian impactites.

THE ZHAMANSHIN STRUCTURE: LITHOPHILE TRACE ELEMENT ABUNDANCES AND STRONTIUM ISOTOPE SYSTEMATICS

J.A.Philpotts[1], S.R.Winzer[2], S.Schuhmann[1], & R.K.L.Lum[3]

1 NASA/Goddard Space Flight Center, Greenbelt, Md.
2 Martin Marietta, 1450 S. Rolling Rd., Balt., Md.
3 University of Maryland, College Park, Md.

The Zhamanshin Structure, U.S.S.R., is of considerable geochemical significance both because of the wide diversity of country-rocks involved in the impact event (clays, sandstones, limestones, schists, quartz-veins, basalts, andesites, etc. - many of which show various degrees of fusion and shock-metamorphism) and also because of the association with these country-rocks of a collection of glasses which includes tektites. We are currently engaged in a systematic study determining Li, K, Rb, Sr, Ba, Ce, Nd, Sm, Eu, Gd, Dy, Er, Yb, Lu, Zr, and Hf abundances and Sr isotopic compositions in these samples. In accord with major element data, some of the dense black glasses (Irhizites) have trace element abundances virtually identical with those in some of the basaltic rock samples. The majority of Irgizites, however, are not only siliceous but have lithophile trace element patterns characteristic of most tektites at the lower level of their reported range. There is only a minor negative Eu anomaly. This pattern is very similar to that of shales. As yet we have not been successful in modelling the compositions of the tektites in terms of analysed country-rock samples. Analysis of further country-rocks, and the study of geochemical indicators of volatilization, including Sr isotope systematics are expected to resolve this difficulty.

ATTACHMENT B

THE PETROLOGY AND GEOCHEMISTRY OF IMPACT MELTS, GRANULITES AND HORNFELSES FROM CONSORTIUM BRECCIA 61175

Stephen R. Winzer[1]

D. F. Nava[2], M. Meyerhoff[1], D. J. Lindstrom[3], R. K. L. Lum[3], M. M. Lindstrom[3], P. Schuhmann[3], S. Schuhmann[2] and J.A. Philpotts[2]

1. Martin Marietta Laboratories, 1450 S. Rolling Road, Baltimore, Maryland 21227

2. Astrochemistry Branch Laboratory for Extraterrestrial Physics, Goddard Space Flight Center, Greenbelt, Maryland 20771

3. Department of Geology, University of Maryland, College Park, Maryland 20742

Revised June 7, 1977

ABSTRACT

Clasts and matrix from consortium breccia 61175 have been analyzed for major, minor and trace elements. Detailed petrographic analyses of 58 clasts have been completed. The matrix of 61175 is anorthositic in composition, with lithophile trace element abundances from 20 to 40 X chondrites. Clasts comprise impact melt rocks, xenocryst and xenolith-free VHA and anorthositic basalts, anorthosite, and ANT granulites and hornfelses. The VHA and anorthositic basalts are interpreted as impact melts, and all are probably formed by impact into anorthositic or anorthositic gabbro target rocks and their matamorphic equivalents. Hornfelses were probably formed by incorporation of breccias or pre-existing melt rocks into a melt sheet prior to cooling. Melt-rock lithophile trace element abundances range from very low, with patterns similar to the anorthosites, to higher abundances with patterns resembling Apollo 16 KREEP. This range may be indicative of more than one melt sheet.

INTRODUCTION

Lunar sample 61175 is a light matrix polymict breccia collected at Station 1 near the rim of Plum crater, Apollo 16 landing site. As described and classified by LSPET (1972) it is one of a small number of samples containing the widest variety of clasts of any breccia type returned from the site (Fig. 1). Because of the variety of rock types present as clasts, this rock was designated for consortium study, and, early in 1976, such a consortium effort was organized. The Principal Investigators of the consortium are E. Anders, J. Geiss, D.F. Nava, O.A. Schaeffer and M. Tatsumoto.

Figure here

The consortium study is being directed by the senior author.

61175 is of more than usual interest because of the variety of rock types present as clasts, and because at least three major processes are indicated by the clasts. Major rock types include extrusive and plutonic igneous rocks, impact melts, and fine and coarse-grained metamorphic rocks (hornfelses and granulites). Almost all rock types described as single specimens or in breccias and rake samples from other stations at the Apollo 16 site are represented in the clast population of 61175. This paper describes the major rock types found in 61175, and discusses their petrologic implications. In addition, major, minor and lithophile trace element data are presented for the bulk rock and two major clast types separated and designated for detailed consortium study (age, isotopic systematics and volatile trace element analysis).

MATRIX

The friable matrix of 61175 consists chiefly of comminuted mineral fragments, from several millimeters down to several microns in size. The mineral fragments are held together by a network of glass, which probably comprises less than 5% of the total mass of the boulder (See Fig. 2). The glass is compositionally heterogeneous with matrix network glasses occasionally showing elevations in Na and K contents relative to Na and K contents in mineral fragments or lithic clasts.

Figure 2 here

Table 1 presents modal data for five polished electron microprobe mounts made from large (several grams each) chips resulting from further cutting of 61175,19. Modes from the five mounts reflect the variability in

Table 1 here

distribution and size of lithic clasts of the major rock types present. Grouped under breccias are a range of rock types including cataclastic ANT breccias, melt rocks and the fine-grained metamorphic rocks (hornfelses). The latter are included among the breccias because, apart from their recrystallized, equilibrated matrices, they closely resemble the melt rocks optically, and cannot always be identified with certainty in the absence of chemical information. Likewise, granulites, which comprise the bulk of the coarse-grained rocks of the ANT suite, are grouped with their respective unmetamorphosed ANT suite rocks.

Lithic clasts comprise up to 45% of the breccia boulder sections, but average about 20%. These clasts were defined somewhat arbitrarily on the basis of the number of mineral grains included in the clast, thus coarse-grained fragments with only three or four crystals were not classified as rock types, whereas fine grained lithic fragments 0.5 to 1 mm in size were often considered classifiable. This arbitrary classification tends to bias the mode towards finer grained rock types, as the coarse-grained ANT rock types would have to be several millimeters in largest dimension to be classifiable. Another caveat to be considered when using these modes is the distinction between basalts and impact melts. All rocks classified as impact melts contain mineral and/or lithic fragments, some of which have been variable shocked. There are clasts, however, which are texturally and mineralogically similar to the impact melts found in 61175, but which contain no lithic or mineral fragments. As the textures of the fragment free rocks also resemble those of some lunar basalts, they cannot be classified as impact melts with certainty and hence are grouped with the basalts.

Optical, SEM and SEM/EDS examination of the matrix of 61175 suggests several conclusions. First, the matrix is composed of comminuted mineral and lithic fragments of several different rock types, including at least one apparently not represented in the clast populations. Coarse spinel fragments, up to several millimeters in longest dimension, occur scattered throughout the matrix of 61175. Such large spinels are not found in the coarse-grained clast suite. Coarse-grained spinel troctolites are described from other Apollo 16 rocks (Prinz et al., 1973), thus it is possible that this rock type may be the source of these spinels. Second, the lithification temperature of the breccia was not high. Evidence against high temperature lithification includes lack of sintering of mineral and glass fragments, high porosity, lack of devitrification of included glasses and absence of reaction rims around included clasts and mineral fragments. Third, the matrix of 61175 probably contains a significant regolith component, as is suggested by the presence of glass shards and droplets and one or two well-formed chrondrules, Fig. 2d. Fourth, the bulk matrix has lower lithophile trace element abundances than Apollo 16 KREEP and higher abundances than the anorthosites (Fig. 3)

Figure here

CLASTS

Lithic clasts range in size from less than one millimeter up to about 2 cm The majority of the clasts are shocked and brecciated ANT rocks or melt rocks, with basalts, metamorphic rocks and igneous plutonic rocks present in decreasing order of abundance.

Because of the difficulties encountered in identifying basalts and melt rocks, the two are grouped together under the superheading "Rapidly cooled igneous rocks." Slowly cooled (plutonic) igneous rocks and their metamorphic equivalents and the hornfelses are discussed separately.

RAPIDLY COOLED IGNEOUS ROCKS

Basalts

The difficulty in differentiating basalts and melt rocks on the basis of texture and mineralogy has already been noted. Many clasts which texturally resemble lunar basalts have bulk and mineral compositions similar to the impact melts, but lack lithic clasts and mineral fragments commonly found in those rocks classified as impact melts. Where field relations are unknown, the distinction between clast-free impact melts and internally derived extrusive rocks is probably impossible without extensive mineralogical, chemical and isotopic data. The following guidelines have been used when classifying clasts from 61175. 1) Rocks which contained Fe metal with 4% or more Ni were classified as impact melts if they also contained xenocrysts and/or xenoliths. 2) Fine-grained rocks which contained magnesian spinel and magnesian olivine (Fo_{70} or greater) were classified as impact melts as this is an unlikely assemblage in basalts. It should be realized that all of these rocks may be impact melts and that application of the term basalt to these rocks is a convenience justified by their texture, but without genetic implications.

Fig. 4 shows the range of textures and mineralogy found in basalt clasts from 61175. Clasts fitting the criteria outlined above show a con-

siderable range in texture and mineralogy. Hyalocrystalline rocks consisting of euhedral plagioclase laths in glass of pyroxene composition (Fig. 4a) form one extreme, while holocrystalline varieties with a microdiabasic texture (Fig 4b) form the opposite extreme. Most basalts are holocrystalline rocks containing plagioclase, clinopyroxene, orthopyroxene, olivine and ilmenite (Fig 4c). Most also exhibit a complex mesotasis which contains one or two pyroxenes, ilmenite, metallic iron, zircon or a mineral with a high zirconium content, sodic plagioclase, apatite and occasionally K-feldspar or glass. All larger clasts with basaltic textures and mineralogy are high alumina, low titania basalts.

Figure 4 here

Pyroxene compositions from basalt clasts are presented in Fig 5. Most pyroxenes are zoned, generally from low Ca, En 55-60 to higher Ca, En_{45-50}. The most extreme zoning observed in a single crystal is from Wo_7En_{72} to $Wo_{14}En_{57}$, and the pyroxene compositions in that rock range from $Wo_7En_{72}Fs_{21}$ to $Wo_{28}En_{27}Fs_{45}$. Pigeonites are most commonly zoned while augites occur as smaller grains with restricted compositional ranges. Olivines are not significantly zoned. Typical zoning ranges from two to four mol % (Fig. 5). Plagioclase compositions in all basalts generally range from An_{90-97}, with larger phenocrysts zoned up to five mol % ($An_{97} \longrightarrow An_{92}$).

Figure 5 here

The chief differences among the basalt clasts analyzed appear to be in degree of crystallinity, texture, crystallization history and the nature of the liquidus phase. Plagioclase is the principal liquidus mineral; however, in a few cases, olivine has clearly crystallized first on the basis of textural evidence. Plagioclase is most often followed by pyroxene or ilmenite but in

some cases both crystallized together. The different crystallization histories create a textural series ranging from hyalocrystalline through intersertal to intergranular and, more rarely, subophitic. A few of the more coarsely crystalline basalts exhibit a diabasic texture, with microphenocrysts of zoned plagioclase (An_{97-92}) in a groundmass of euhedral plagioclase laths, subhedral pyroxene, olivine and ilmenite (Fig. 4c). The more coarsely crystalline rocks lack the complex mesostasis regions found in the fine-grained intersertal basalts.

Several conclusions can be made regarding the basalt component of 61175: 1) All the basalts appear to be the high Al_2O_3, low TiO_2 variety (when large enough to be classified reliably). Most fall into the field of anorthositic basalts as defined by Irving (1975). 2) They form two groups on the basis of crystallization history, those which crystallized plagioclase first and those which crystallized olivine first. 3) Their pyroxene and olivine compositions are either similar to or slightly more magnesian than the high Al_2O_3, low TiO_2 basalts described in other Apollo 16 samples (e.g. Delano, 1975). 4) The wide range of textures either indicates differing cooling histories or nucleation rates for the basalts present.

Impact Melt Rocks

By far the most common, and most variable, suite of clasts found in 61175 are the impact melt-rocks. Impact melts range in texture and composition from glasses to holocrystalline rocks in which the groundmass texturally and mineralogically resembles the basalts (Fig. 6). Glass shards, or fragments of glass and maskelynite up to 5 mm in longest dimension are present (Fig. 6a). These glasses have compositions similar to those of

Figure 6 here

plagioclase found in the clasts (Fig. 7). Other glasses occur as devitrified melt with few mineral fragments to devitrified fragment-laden melts (the fine grained hyalocrystalline melt rocks) (Fig. 6b). The crystalline or partly crystalline melt rocks range in texture from wispy fine-grained hyalocrystalline melts with acicular to subhedral plagioclase, often with glass cores and familiar "swallow tail" configureation (Fig. 6c) to fragment-laden microdiabases with euhedral feldspar phenocrysts and a ground mass of euhedral to subhedral plagioclase, low calcium pyroxene, pigeonite and olivine. The plagioclases occur as either subradial growths or as subaligned to aligned laths suggestive of flowage (Fig. 6b). Many melt rocks contain opaque phases which are concentrated in patches (Fig. 6d) of anhedral grains of Fe (up to 9% Ni), troilite, ilmenite and occasionally a phosphide (schreibersite?).

Figure 7 here

Xenocrysts include plagioclase, olivine and, more rarely, pyroxene. A few of the melt rocks contain xenoliths, usually as very small polycrystalline aggregates. One such xenolith has an annealed texture, but others retain igneous textures. Xenocryst and xenolith populations range from zero to more than 50% of the total clast.

Pyroxene and olivine compositions from melt rock clasts are presented in Fig. 8. Pyroxene compositions generally overlap those of the basalts found as clasts in 61175, as do the olivines. In most melt rocks, groundmass pyroxenes and olivines are quite magnesian (Fo_{70} or higher (to Fo_{95}), En_{70-80} for low Ca pyroxene). Plagioclases generally range from An_{88} to An_{95}, but sodic plagioclase occurs occasionally. K-feldspars, apatite and whitlockite are rare or absent.

Figure here

Accessory phases include magnesian spinel, chromite, troilite, Fe(Ni) metal, schreibersite, ilmenite, armalcolite, a zirconium mineral and rutile. Accessory phases are not always found in the mesostasis, but may occur as individual grains scattered throughout the rock, or in aggregates concentrated in certain areas of a clast. The texture of some of these aggregate areas suggests that they result from breakdown and melting of xenoliths, thus some of the accessory phases may not have crystallized from the melt formed by the impact.

PLUTONIC ROCKS AND METAMORPHIC EQUIVALENTS

Few pristine plutonic igneous clasts are found in 61175. Most rocks of the ANT suite are recrystallized or brecciated, thus obscuring original textures and making rock classification difficult. Both granulites and igneous rocks are grouped together in this section for convenience A few of the coarse-grained diabases or micro troctolites are included with the plutonic rocks (Fig. 9a), but the most common plutonic rock is anorthosite, which occurs as larger clasts up to 2 cm long (Fig. 9b). The anorthosites have been subjected to shock pressures up to the plagioclase/maskelynite transition, and some have been shocked to the point where some melting has occurred. Plagioclase in anorthosites is coarse-grained (to several mm), and has compositions between An_{95} and An_{100}. Minor and accessory minerals include magnesian olivine, orthopyroxene, and occasionally ilmenite or spinel.

Figure here

More commonly found are coarse-grained granulitic anorthosites, norites or troctolites. These clasts exhibit a range of metamorphic textures,

including granular anhedral groundmass plagioclase exhibiting smooth boundaries and triple-junctions indicative of an equilibration during subsolidus recrystallization (Fig. 9c). Included in this groundmass are anhedral, irregular orthopyroxene poikiloblasts which enclose anhedral plagioclase, and, rarely, ilmenite (Fig. 9d). In several clasts, these orthopyroxene poikiloblasts have exsolved a high calcium pyroxene as lamellae up to 0.1 mm wide (Fig. 9d). The composition of the major minerals in any one granulite clast is usually quite constant. Generally, olivine and pyroxene are unzoned, plagioclase is often unzoned but euhedral to subhedral grains are occasionally found to have more calcic cores and more sodic rims. Anhedral plagioclase grains are occasionally found enclosing small rounded olivine grains, or euhedral ilmenites. Larger anhedral magnesian ilmenites are found in some clasts.

Pyroxene and olivine compositions from plutonic igneous and granulitic ANT rocks (Fig. 10) exhibit a very small range in composition. Figure 10 here

Olivines range from $Fo_{67} \longrightarrow Fo_{72}$, pyroxenes range from $Wo_5En_{67}Fs_{28} \longrightarrow Wo_5En_{71}Fs_{24}$ and $Wo_{35\text{-}40}\ En_{48\text{-}46}Fs_{17\text{-}14}$ in one clast, to $Wo_{4\text{-}10}En_{67\text{-}60}Fs_{28\text{-}33}$ and $Wo_{25\text{-}45}En_{56\text{-}38}Fs_{13\text{-}19}$ (as lamellae in the low Ca pyroxene).

The texture and restricted range of compositions of the minerals from the recrystallized ANT rocks is indicative of high temperature metamorphism. The textures and grain sizes are comparable to terrestrial granulites, and are, by inference, the result of a rather long residence time at high temperatures. Metamorphism has been sufficiently thorough to reduce chemical gradients between minerals and within minerals. The presence of such thoroughly metamorphosed rocks raises several interesting questions about the lunar crust at the Apollo 16 site. These will be discussed in the conclusions.

HORNFELSES

The hornfelses are a group of clasts characterized by textural variety and chemical homogeneity Superficially, some of the hornfelses resemble the melt rocks, however certain textural differences may be discerned The typical hornfels texture is one of anhedral to subhedral plagioclase porphyroblasts or xenocrysts surrounded by anhedral olivine or pyroxene (or both) and plagioclase. These anhedral grains form an interlocking mass which, when viewed at moderate magnification with a scanning electron microscope, exhibit smooth curving boundaries and triple junctions (Fig. 11). This basic texture has several varieties, one of the more important of which is the development of porphyroblastic pyroxenes in the groundmass surrounding the xenocrysts (or xenoliths). Where this texture is best displayed, large subhedral to euhedral pyroxene porphyroblasts enclose plagioclase xenocrysts (sometimes subhedral to euhedral) and groundmass plagioclase (anhedral) (Fig. 11c, d). The interstitial areas between the pyroxene porphyroblasts consist of granular olivine and plagioclase with smooth boundaries and triple-junctions This textural type has been found in only one clast so far. Anhedral pyroxene porphyroblasts are more commonly found, but most common are small, anhedral pyroxenes with anhedral olivine or plagioclase inclusions which make up the groundmass along with single anhedral olivines, plagioclases and pyroxene. In the coarse grained porphyroblastic varieties, two pyroxenes have been found. The main porphyroblast is a low Ca pyroxene (often orthopyroxene) hosting small high Ca pyroxenes of irregular shape and size.

Figure 1 here

All hornfelses are characterized by an absence of glass and by chemical homogeneity among the minerals present. Olivines and pyroxenes

are unzoned and of constant composition throughout the clast (Fig. 8), in contrast to olivine and pyroxene compositions from the melt rocks in which considerable chemical heterogeneity is exhibited throughout a single clast. Plagioclase is also generally unzoned and of constant composition, but in the larger crystals and in the xenocrysts, zoning does occur in the form of calcic cores (usually most of the grain) and thin, more sodic, rims The rim composition is usually the same as the composition of the groundmass plagioclase.

Accessory minerals include Fe metal, with the same range of Ni content as the melt rocks (4.5-9%), troilite, ilmenite, occasional apatite and phosphide. Sodic feldspar, K-feldspar and whitlockite are generally absent.

In summary, the hornfelses exhibit an equilibrated texture, lack of zoning and chemical homogeneity among mineral phases, which is indicative of a close approach to chemical equilibrium. In this manner the hornfelses are similar to the coarse-grained granulites. In fact, with the exception of grain size, the textures and mineral compositions of these two groups are remarkably similar.

BULK COMPOSITION

In order to relate the textural types found in 61175 to one another, most of the clasts were analyzed using a defocussed beam technique. These analyses, 58 in all, were done as follows: As with the mineral analyses, a scanning electron microscope with energy dispersive spectometer was used. The microscope was set in scanning mode, and, where possible, the magnification adjusted to include the entire clast. Where irregular clasts

or clasts with prominent cracks or holes were to be analyzed, the analysis was done over several smaller areas and averaged. Three repeat analyses, each with a counting time of 120 sec., were done. This is sufficient to keep the counting error below one percent for all but minor elements. The data were corrected using the Bence/Albee correction procedures and then recorrected following the method outlined by Albee et al, 1977. Comparison of normative mineral compositions with the actual compositions obtained by SEM/EDS analysis shows that the differences between the two are small (one to two mol % An, Fo, En or Wo) for the major mineral components.

The bulk chemical analyses of ANT and granulitic ANT, basalt, melt rocks and hornfelses are plotted on a ternary diagram (Fig. 12) after Walker et al, (1973a). No single group of rocks, classified on the basis of texture and mineralogy, is identifiable on the basis of bulk chemistry. All groups overlap one another, and most lie in the plagioclase primary crystallization field. The majority of rocks analyzed fit the criteria for use of this diagram, including the "basalts". Three clasts, all breccias containing significant glass, have compositions far from the compositional plane of the diagram and are not plotted. The position of rocks in the plagioclase field deserves comment. As indicated earlier, basalts can be divided into two groups based on the liquidus phase (plagioclase or olivine). The same is true for the impact melts, and may be extended to those rocks which apparently crystallized magnesian spinel first. All rocks plotted on this diagram would be expected to have plagioclase as the liquidus phase, under equilibrium conditions. The fact that textural examination reveals the presence of other liquidus phases suggests that other factors, such as undercooling, may be controlling the liquidus phase. Another possibility,

Figure 1 here

considered less likely, is that these phases could be relicts, or were nucleated around relicts as the melts cooled.

Other trends are evident from this plot. First, the basalts are clustered toward the An apex of the triangle, along with the more feldspathic granulites Many hornfelses cluster near the spinel-plagioclase-olivine piercing point, but examples of both basalts and hornfelses can be found throughout the entire range. The melt rocks (excluding breccias and the odd glassy compositions) span the entire range defined by the feldspathic granulites and the most ferromagnesian hornfelses.

A few clasts and matrix samples from 61175 have been separated and analyzed for major elements by semi-micro atomic absorption spectrophotometry (Nava and Philpotts, 1973) (Table 2). Large-ion-lithophile trace element abundances were also obtained on these samples, following the method of Schnetzler et al , (1967). Differences in major element abundances in the separated samples of matrix and clasts analyzed by atomic absorption spectrophotometry mainly reflect different amounts of mafic and feldspathic components, with the matrix being somewhat more mafic than the clasts. Bulk matrix samples analyzed are identical within analytical error (for major elements), and their counterparts are to be found in other Apollo 16 boulders, for instance 67455 fragment laden melt (Lindstrom et al., 1977) and 67435 glass coating (Warner et al., 1976). Counterparts to this composition can be found both at the North Ray and South Ray crater sites. This is not surprising in view of the generally anorthositic nature of the Apollo 16 breccia boulders. The clasts differ from the matrix, and their chemical differences reflect the different rock types involved. Sample 61175,151 is an anorthosite, somewhat shocked and brecciated, and comparable in composition to other

Table 2 here

anorthosite breccias from the Apollo 16 site; 61175,126 is a melt rock compositionally similar to those analyzed by SEM/EDS. It is also similar to the bulk matrix of 61175.

Large-ion-lithophile trace element abundances for separated clasts and matrix are presented in Table 3 and Fig 3. Compared to the matrix compositions for the Apollo 17 boulders, the matrix trace element abundances in 61175 are more variable, and are considerably depleted in KREEP (as discussed earlier). The matrix trace element abundances are higher than those of the more feldspathic breccias such as 67455 (Lindstrom et al., 1977), but are lower in abundance than Apollo 16 KREEP (Hubbard et al., 1973). The matrix LIL trace element abundances are consistent with the modal data, and SEM/EDS data which suggest that the majority of the matrix is anorthositic. Glass, which binds the matrix together, is of variable composition, and is irregularly distributed. As the most potassic compositions come from the glass, it is reasonable to assume that the glass is the major contributor to the KREEP component of the matrix.

Table 3 here

As insufficient number of clasts have been analyzed for trace elements to make firm conclusions about the relationship of clasts to one another, however some general remarks can be made. First, the anorthosite breccias (subjected to shock pressures above the maskelynite phase transition, but below those needed for significant melting) show typical anorthosite lithophile trace element patterns with a range of from 1 to 10x chondrites. More surprising, however, are the low REE abundances in one of the dark melt-rock clasts analyzed (61175,126). This pattern is typical of a highlands anorthosite The rare-earth element abundances in the other dark clast analyzed (61175,133) are higher than the other clasts or matrix analyzed, and approach Apollo 16 KREEP in abundances (Hubbard et al., 1973). The

spread in lithophile trace element abundances between the melt rocks analyzed differs from that of single terrestrial impact melt sheets. In terrestrial impact melts (e.g., Winzer 1975, Winzer and Lum 1975, Floran, et al., in press) the trace element abundances and patterns are usually nearly identical. The same observation can be made for the Apollo 17 melts (e.g , Winzer et al., 1977). The spread in abundances and differences in the patterns for the two melt-rock clasts analyzed may indicate that more than one melt sheet, or more than one impact event is represented in the clast population of 61175. As some of the clasts analyzed by SEM/EDS techniques are low in K, they may also be low in REE's and may represent an impact melt with a very low KREEP component. Another possible explanation which cannot be discounted, is that of sample heterogeneity. Both melt rock clasts are quite small, and, although they are individual clasts from different parts of 61175, they may not be representative of any given melt-sheet composition.

DISCUSSION

The clasts in 61175 exhibit a remarkable textural diversity yet, when bulk composition and mineral compositions are compared between groups of samples, this diversity tends to disappear. Unlike other major lunar highlands samples, whose clasts differ significantly in chemical composition (e.g., Winzer et al., 1977; James, 1977) no group of clasts in 61175 appears distinct from another except on the basis of texture. All mineral compositions from the various clast types overlap one another, and only those clasts with a metamorphic texture form a distinct group on the basis of their restricted mineral compositions. This restricted group is a sub-group of all other clasts in terms of mineral composition.

The simplest explanation for these similarities is that all igneous textured rocks except the ANT suite rocks are impact melts whereas the hornfelses are their metamorphosed equivalents. There is no doubt that the melt-rocks, as described in the earlier portion of this paper, are of impact origin. The more difficult assertion to prove is that those rocks with basaltic textures, free of xenoliths or xenocrysts, are also impact generated melt rocks.

Evidence in favor of such an interpretation is indirect, but suggestive. First, all igneous textured, xenolith and xenocryst-free rocks plot in either the anorthositic basalt or VHA basalt fields delineated by Irving (1975). They are similar or identical in composition to coarse-grained igneous rocks of the highlands ANT suite. Experimental studies on anorthositic basalts and VHA basalts (such as 68415 Walker et al., 1973[a;b]) indicate that these compositions would have plagioclase, spinel and corundum on the liquidus at 15 kb, and this assemblage contradicts that derived from basalt parent materials. It was judged more likely that this type of rock represented shallow melting of plagioclase cumulates. Second, those clasts which do contain iron metal show a nickel abundance which is considerably higher than that of iron metal in mare basalts. Such elevations (generally up to 9% Ni in these rocks) are usually considered to be indicative of meteoritic origin (e.g , Hewins and Goldstein, 1975). Siderophile trace element abundances for these clasts should help in their interpretation Third, the bulk compositions of the melt rocks and "basalts" and the compositional ranges of their major mineral phases are identical. Detailed petrological studies of terrestrial impact melts (e.g., Grieve 1975; Floran, et al., in press) indicate that rocks with highly variable textures can be

formed by the crystallization of melts with relatively constant composition. Winzer (1975), Winzer et al., (1976, 1977) and Grieve (1975) have established that impact melts have major and trace element compositions explainable in terms of total melting and mixing of target rocks. The compositional similarities of impact melts and "basalts" to ANT suite rocks found as clasts in 61175 suggest that both are impact generated total melts derived from such rocks. The presence of xenoliths and xenocrysts of ANT rocks in the impact melts supports this hypothesis, as do the trace element abundances.

On the basis of the evidence cited above, we favor the hypotheses that all non-plutonic, igneous-textured rocks are impact melts. The possibility still exists, however, that the basaltic-textured rocks originated by internal processes, such as shallow partial melting, however such processes seem unlikely. Age dating and lithophile trace element data for these clasts should help resolve the problem of their origin.

The origin of the metamorphic rocks remains to be explained. Considerable controversy has arisen over the origin of the fine-grained rocks containing sieve-textured pyroxenes. Depending on interpretation, these rocks have been variously labelled poikilitic (e.g., Simonds et al., 1973) or poikiloblastic (e.g., Albee et al., 1973). More recently, poikilitic pyroxenes have been reported from terrestrial impact melts (Grieve, 1975, Floran et al., in press), but poikilitic plagioclase is more common Experimental studies (Lofgren, 1977) suggest that poikilitic textures can be formed under restricted conditions of nucleation and under-cooling. These poikilitic melts have several textural features in common with one another, the most important of which are the dominance of euhedral to subhedral feldspars, as found in poikilitic pyroxenes, and the presence of euhedral to subhedral

crystalline material in the groundmass surrounding the poikilitic minerals The groundmass may be glassy or completely crystalline.

The 61175 hornfelses, unlike the poikilitic rocks from terrestrial melts, and Apollo 17 poikilitic rocks lack the dominant euhedral to subhedral plagioclases found as inclusions in the pyroxenes. Those hornfelses not containing sieved pyroxenes have a granular texture, with anhedral to subhedral plagioclase, pyroxene and olivine. The texture ranges through rocks containing pyroxenes or olivines with inclusions of plagioclase and/or pyroxene or olivine through those with larger, sieve like pyroxenes including anhedral (usually round) olivine and anhedral to subhedral plagioclase. The interstitial material in all hornfelses is characterized by anhedral to subhedral plagioclase and pyroxene and anhedral olivine. These minerals form the granular base, with 120° intersections indicative of textural equilibration by subsolidus recrystallization. The base texture is not reported from any of the poikilitic impact melts, although recrystallization is evident in partially digested clasts in the Manicouagan impact melt (Floran et al., in press). On the basis of the dominant crystal form of included minerals and interstitial groundmass in the 61175 hornfelses these rocks must have undergone considerable subsolidus recrystallization, and thus the textures observed are considered to be dominantly metamorphic. The textures are thus termed poikiloblastic where larger pyroxene grains have formed

Euhedral to subhedral feldspars do occur in the poikiloblastic rocks, as well as in the granoblastic hornfelses. Most of these are clearly xenocrysts, but occasional laths occur in the groundmass. These plagioclases generally have the same composition as those which are anhedral, thus they appear to be chemically equilibrated with the rest of the rock. It is

uncertain whether these are xenocrysts, or whether their form is controlled by the subhedral mafic phases. Euhedral to subhedral plagioclase and other minerals are not uncommon in metamorphic rocks (see Spry, 1969 plates 15, 18, 21 and 23 for examples), thus their presence does not exclude a metamorphic origin.

The presence of xenocrysts in the hornfelses is strong evidence that the original material could have been an impact generated melt rock. Another possibility, which has been raised by Bence et al., (1973) and Albee et al , (1973), is that the original rock was a glassy breccia or agglutinate and that temperatures were sufficiently high to cause partial melting of the original rock. Evidence for this hypothesis includes the presence of euhedral crystals, and the absence of less refractory phases such as pyroxene among the xenocrysts This explanation cannot be excluded with the evidence presently available.

If partial melting is an important process in the origin of the poikiloblastic rocks, it could be an important factor in producing both the coarse-grained granulitic rocks and the fine-grained hornfelsic rocks. The poikiloblastic granulites differ only in grain size from the hornfelses, the textures are similar or identical, as are the mineral compositions. There is considerable evidence from large terrestrial melt sheets that digestion or partial digestion of even very large lithic clasts can occur. This process is similar to anatexis in high-grade metamorphic terranes, and is a combination of metamorphic and igneous processes, producing textures indicative of both subsolidus recrystallization and melting. The chief drawback to the clast digestion process is that, more often than not, the melt which is formed in the clast remains as a glass and does not recrystallize. In addition, no

coarse-grained rocks equivalent in texture to the granulites have been found in included clasts in terrestrial melt sheets. Evidence from regional metamorphic terrains suggests that development of such textures requires long time periods at high temperatures. Insufficient data exist to quantify either the cooling times for large melt sheets, or the actual time needed to form the coarser-grained granulitic textures, thus the plausibility of this hypothesis cannot be quantitatively evaluated.

CONCLUSIONS

On the basis of the available evidence, the different lithotypes found in 61175 can be explained by a multi-stage process. The first stage would be formation of a relatively large melt sheet(s) by impact(s) into highland ANT suite rocks. These impacted rocks may include granulites which are metamorphic equivalents of the original ANT rocks formed by processes akin to terrestrial regional metamorphism prior to impact (see Winzer, 1976). As the melt expanded radially outward from the point of impact it would have swept up and included clasts of original country rock, and breccias formed during the impact. The melt would solidify, forming a variety of textures according to its proximity to cold country rock and the size and number of included xenocrysts and xenoliths Included breccia or possibly pre-existing melt rock clasts would undergo high temperature thermal metamorphism possibly including extensive partial melting following their inclusion in the melt. Following solidification of the melt, and final cooling, the resulting melt sheet was again the target of an impact, which possibly formed the 61175 breccia from melt sheet and regolith components. More than one melt sheet may have been involved, as suggested by the limited trace element data available,

Acknowledgement

This research was partially supported by NASA/GSFC contract NAS 5-23544 to Martin Marietta Laboratories and grant NSG 5121 to the University of Maryland. The manuscript benefitted from helpful reviews by R. J. Floran and U. B. Marvin.

References

Albee, A. L., Gancarz, A. J. and Chodos, A. A. (1973) Metamorphism of Apollo 16 and 17 and Luna 20 metaclastic rocks at about 3.95 AE Samples 61156, 64423,14-2, 65015, 67483,15-2, 76055, 22006 and 22007. Proc. Lunar Sci. Conf. 4th, p. 569-595.

Albee, A. L., Quick, J. E. and Chodos, A A (1977) Source and magnitude of errors in "broad-beam analysis" (DBA) with the electron probe (abstract). In Lunar Science VIII, p. 7-9. The Lunar Science Institute, Houston.

Bence, A. D., Papike, J. J., Sueno, S and Delano, J. W. (1973) Pyroxene poikiloblastic rocks from the lunar highlands. Proc. Lunar Sci. Conf. 4th, p 597-611.

Delano, J. W. (1975) Petrology of the Apollo 16 mare component. Mare Nectaris. Proc. Lunar Sci. Conf. 6th, p. 15-47.

Floran, R. J., Grieve, R. A. F., Phinney, W. C., Warner, J. L. Simonds, C H. and Blanchard, D. P. (in press) Manicouagan impact melt, Quebec. PartI: Stratigraphy, petrology and chemistry.

Grieve, R. A. F. (1975) Petrology and chemistry of the impact melt at Mistastin Lake crater, Labrador. Geol Soc. Amer. Bull. 86, p. 1617-1629.

Hewins, R. H. and Goldstein, J. I. (1975) The provenance of metal in anorthositic rocks (abstract) In Lunar Science VI, p. 385-360. The Lunar Science Institute, Houston.

Hubbard, N. J., Rhodes, J. M., Gast, P. W., Bansal, B. M., Shih, C. Y., Weismann, H and Nyquist, L. E. (1973) Lunar rock types: The role of plagioclase in non-mare and highland rock types. Proc Lunar Sci Conf. 4th, p. 1297-1312.

Irving, A. J. (1975) Chemical, mineralogical and textural systematics of non-mare melt rocks: Implications for lunar impact and volcanic processes, Proc. Lunar Sci. Conf. 6th, p. 363-394.

James, O. B. (1976) Petrology of aphanitic lithologies in consortium breccia 73215. Proc. Lunar Sci. Conf. 7th, p. 2145-2178.

LSPET (1972) Preliminary examination of lunar samples. In Apollo 16 Preliminary Science Report, NASA SP-315. 7-1-7-58.

Lindstrom, M.M., Nava, D.F., Lindstrom, D.J., Winzer, S.R., Lum, R.K.L., Schuhmann, P.J., Schuhmann, S. and Philpotts, J.A. (in press) Geochemical studies of the white breccia boulders at North Ray Crater, Descartes region of the Lunar Highlands.

Lofgren, G.E. (1977) Dynamic crystallization experiments bearing on the origin of textures in impact generated liquids (abstract) In Lunar Science VIII, p. 589-590. The Lunar Science Institute, Houston.

Nava, D.F. and Philpotts, J.A. (1973) A lunar differentiation model in light of new chemical data on Luna 20 and Apollo 16 soils. Geochim. Cosmochim. Acta 37, p. 963-973.

Prinz, M., Dowty, E., Keil, K. and Bunch, T.E. (1973) Spinel troctolite and anorthosite in Apollo 16 samples. Science 179, p. 74-76.

Schnetzler, C.C., Thomas, H.H. and Philpotts, J.A. (1967) Determination of rare-earth elements in rocks and minerals by mass spectrometric stable isotope dilution technique. Anal. Chem. 39, 1888-1890.

Simonds, C.H., Warner, J.L. and Phinney, W.C. (1973) Petrology of Apollo 16 poikilitic rocks. Proc. Lunar Sci. Conf. 4th, p. 613-632.

Spry, A. (1969) Metamorphic Textures Pergamon Press, Oxford 350 pp.

Walker, D., Longhi, J., Grove, T.L., Stolper, E.M. and Hays, J.F. (1973a) Experimental petrology and origin of rocks from the Descartes Highlands. Proc. Lunar Sci. Conf. 4th, p. 1013-1032.

Walker, D., Longhi, J., Grove, T.L., Stolper, E.M. and Hays, J.F. (1973b) Origin of Lunar Feldspathic rocks. Earth and Planet Sci. Lett. 20, p. 325-336.

Warner, R.D., Planner, H.N., Keil, K., Murali, A.V., Ma, M.S., Schmitt, R.A., Ehmann, W.D., James, Jr., W.D., Clayton, R.N. and Mayeda, T.K. (1976) Consortium investigation of breccia 67435. Proc. Lunar Sci. Conf. 7th, p. 2379-2402.

Winzer, S.R. (1975) Does impact produce chemical fractionation? (abstract) EOS (Trans. Amer. Geophys. Union) 56, p. 389-390.

Winzer, S.R. (1976) Studies of consortium breccia 61175 (abstract) Meteoritics 11, p. 390-393.

Winzer, S.R., Nava, D.F., Schuhmann, S., Lum, R.K.L., and Philpotts, J.A. (1975) Origin of the Station 7 Boulder. A note. Proc. Lunar Sci. Conf. 6th, p. 707-710

Winzer, S.R., Nava, D.F., Schuhmann, P.J., Lum, R.K L., Schuhmann, S., Lindstrom, M.M., Lindstrom, D.J. and Phılpotts, J.A. (1977) The Apollo 17 "Melt Sheet": Chemıstry, age and Rb/Sr systematıcs. Earth and Planet Sci. Lett. 33, p. 389-400.

TABLE 1

Modal Analysis of Thin Sections From 61175

Sample #	61175,9	61175,101	61175,104	61175,95	61175,98	(Average All Section
01	4.6	3.9	6.1	2.1	4.5	4.4
Plag	66.8	77.7	68.2	52.8	72.5	67.7
Opx	0.2	0.6	0.06	---	0.5	0.2
Cpx	0.04	---	0.9	0.05	0.05	0.2
Ilm	0.04	0.03	0.3	0.11	0.05	0.15
Clasts						
Basalt	7.0	9.1	9.1	4.5	7.2	7.5
Breccia	14.3	5.1	11.2	37.3	12.2	14.8
Anorthosite	4.6	2.8	2.0	1.4	2.4	3.0
Norite	1.8	0.03	0.9	0.13	0.1	0.7
Troctolite	0.7	0.03	1.4	1.6	0.6	1.0
Number of Points	6324	3877	5315	3785	1952	21253

TABLE 2

Major and Minor Element Abundances
in Clasts and Matrix from 61175

Sample	61175,126 Dark Clast	61175,151 White Clast	61175,147 Matrix	61175,168 Matrix
SiO_2	45.5	44.6	45.5	45.6
TiO_2	0.47	0.47	0.53	0.52
Al_2O_3	28.78	30.29	27.88	27.87
FeO	3.38	2.80	4.33	4.25
MnO	0.05	0.04	0.06	0.06
MgO	4.46	3.14	4.88	4.76
CaO	16.75	16.16	16.14	16.19
Na_2O	0.58	0.56	0.51	0.50
Cr_2O_3	0.05	0.04	0.06	0.06
Total	100.02	98.10	99.89	99.81

TABLE 3

Lithophile Trace Element Abundances
in Matrix and Clasts from 61175

mple	61175,126 dark clast	61175,131 white clast	61175,133 dark clast	61175,147 matrix	61175,151 white clast	61175,167 matrix	61175,168	61175,170 white clast	BCR-1
Li	4.80	4.98	11.5	10.1	4.48	6.50	7.37	2.00	12.4
K	318	504	1800	1050	244	666	794	36.1	13600
Rb	0.636	1.57	5.41	2.97	0.437	1.64	2.19		49.0
Sr	200	174	149	246	219	177	182	163	332
Ba	45.7	65.3	280	153		91.8		8.34	663
Ce	5.87	11.4	76.0	33.0		18.9		0.541	53.2
Nd	4.18	7.05	48.2	21.1		11.8		0.392	28.7
Sm	1.17	2.04	13.2	5.91		3.37		0.144	6.40
Eu	1.19	1.03	1.50	1.66		1.20		0.695	1.85
Gd									
Dy	1.85	2.97	16.6	8.41		4.40		0.155	
Er	1.09	1.75	9.94	4.69		2.59		0.104	3.60
Yb	1.01	1.67	9.06	4.29		2.51		0.095	3.37
Lu	0.152	0.226	1.27	0.654		0.347		0.108	0.446
Zr						194			
Hf									
eight	0.02347g	0.03894	0.01709	0.13265	0.0702	0.07355	0.11954	0.01343	0.11339

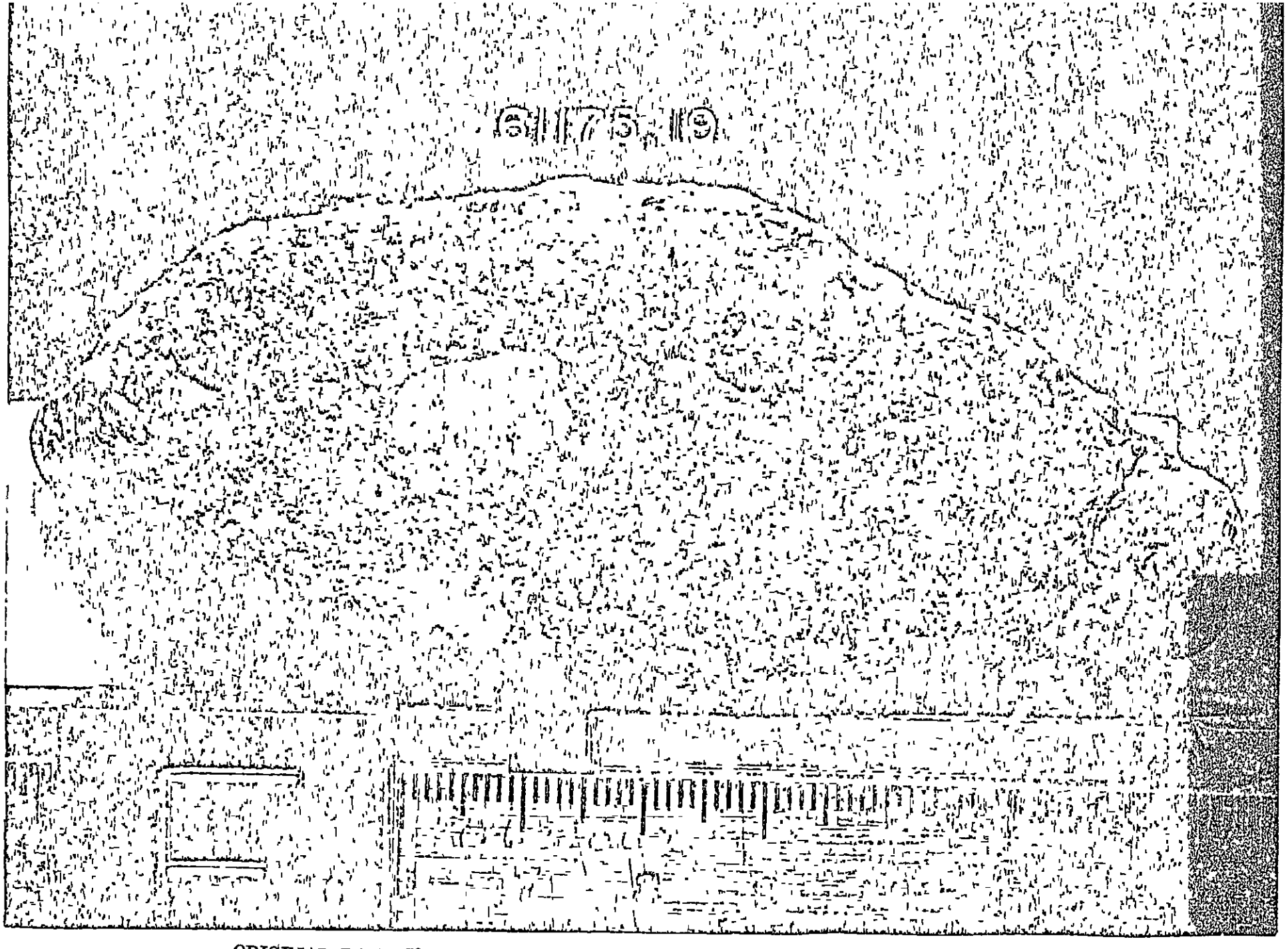

ORIGINAL PAGE IS
OF POOR QUALITY

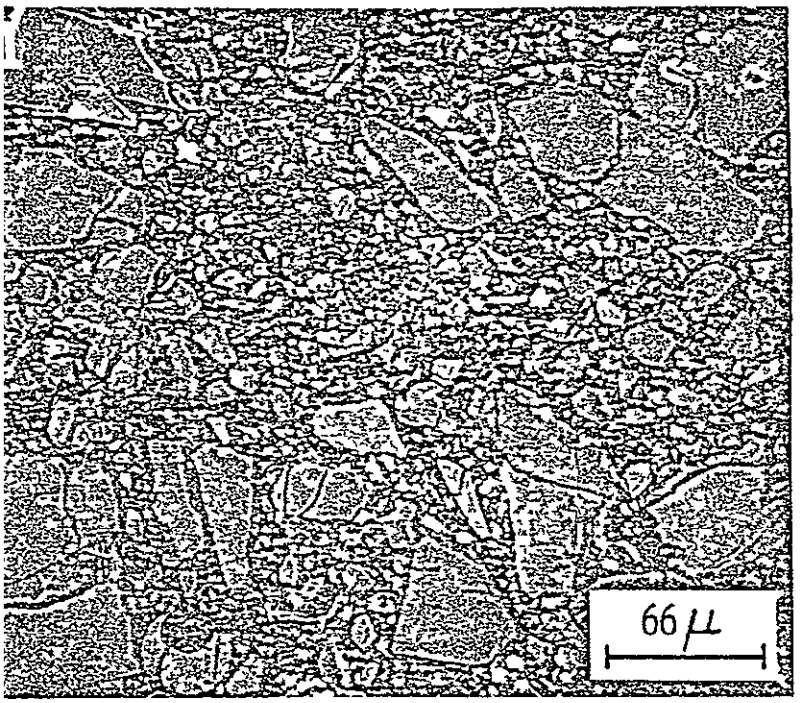

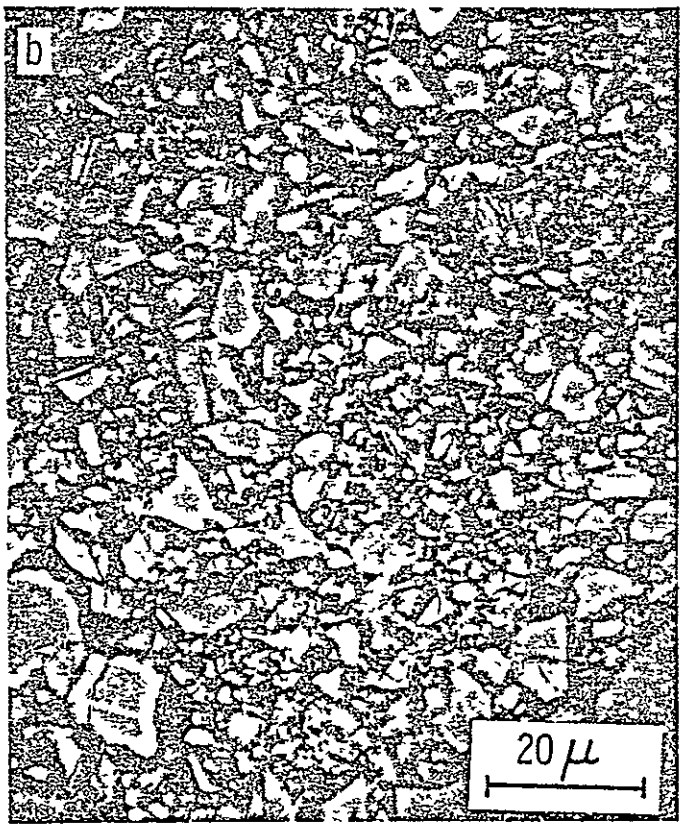

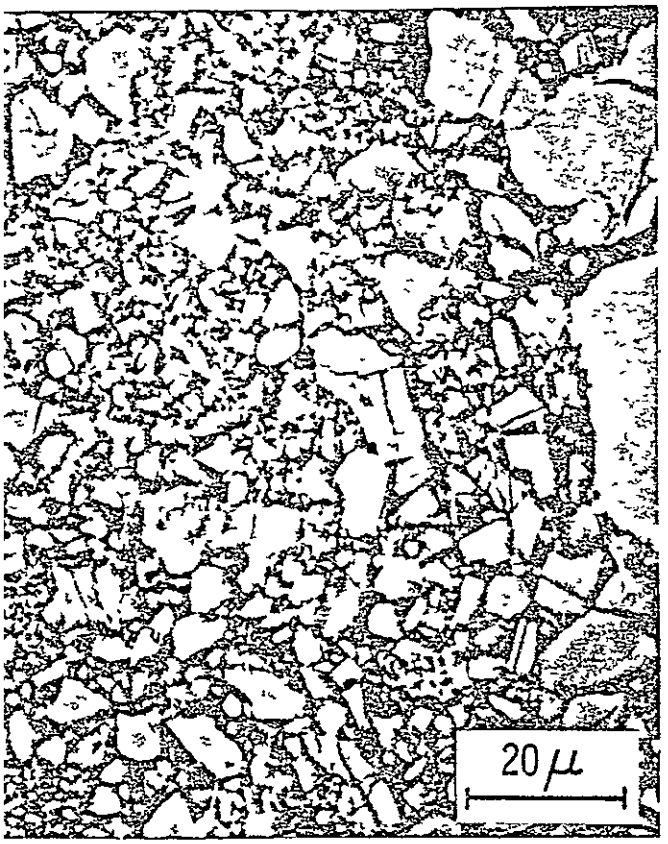

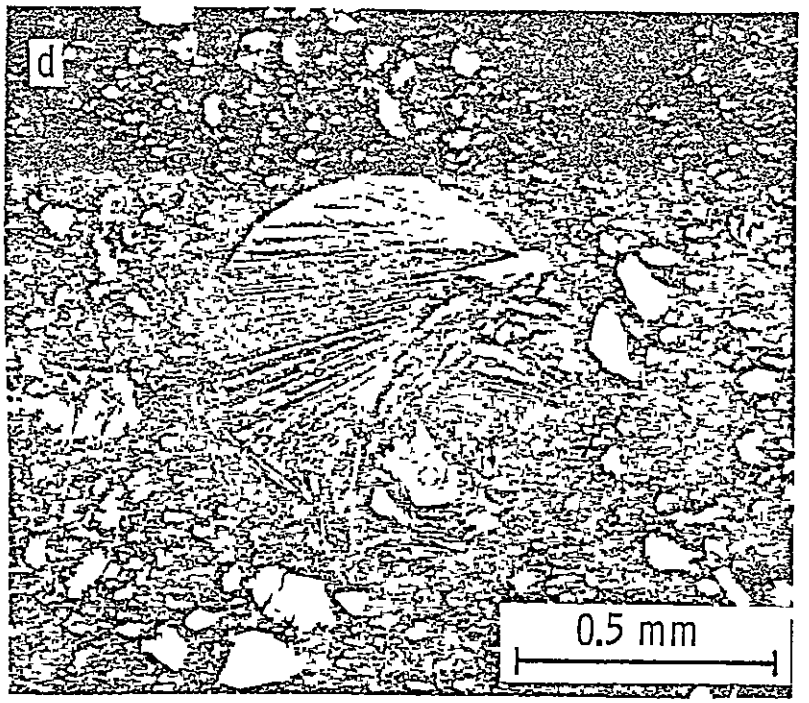

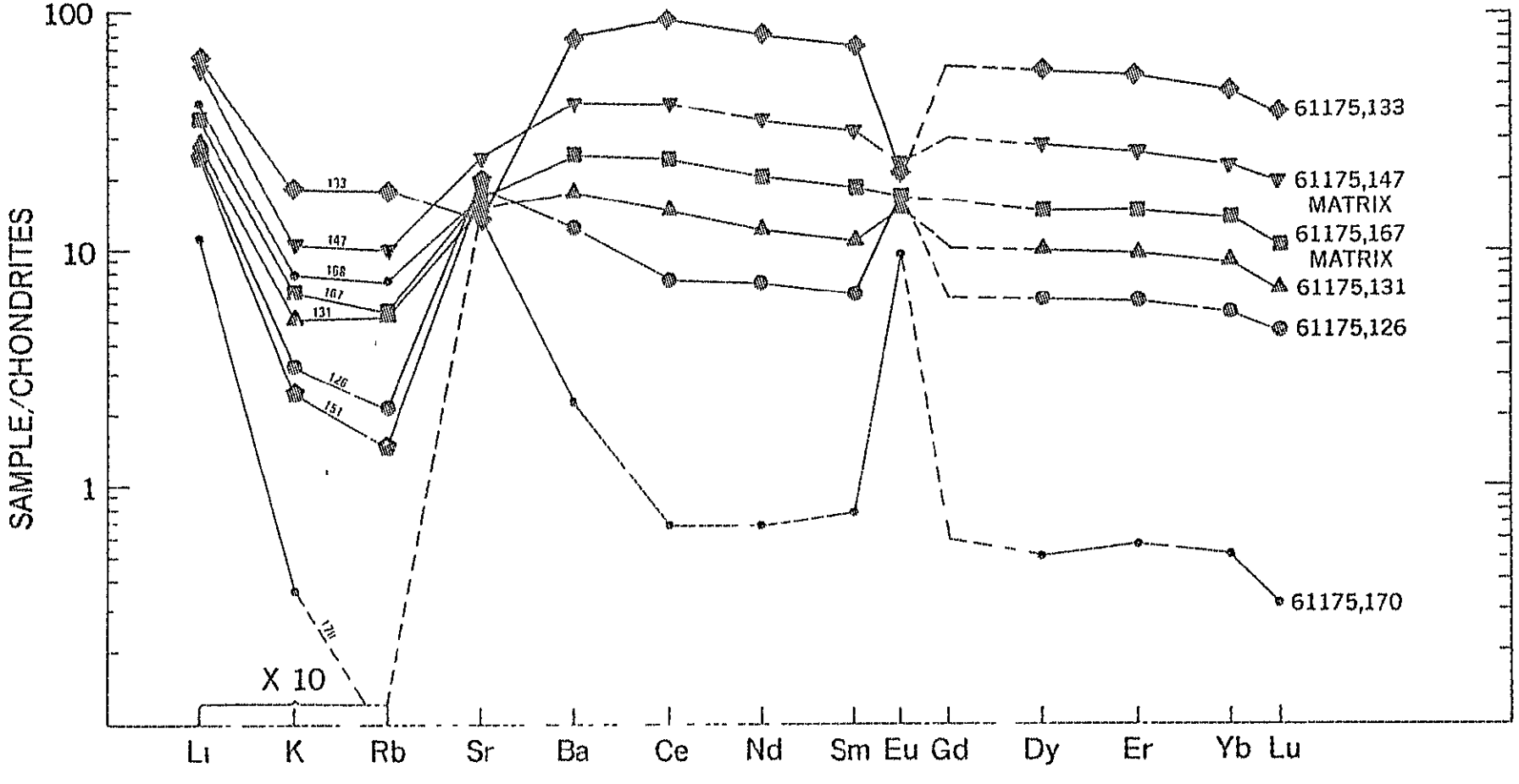
100
10
1
SAMPLE/CHONDRITES
X 10
Li
K
Rb
Sr
Ba
Ce
Nd
Sm
Eu
Gd
Dy
Er
Yb
Lu
61175,133
61175,147
MATRIX
61175,167
MATRIX
61175,131
61175,126
61175,170

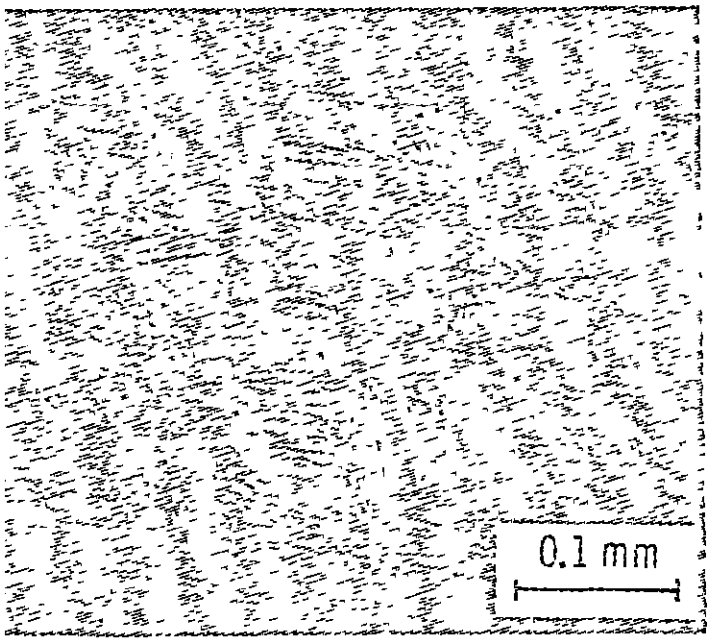

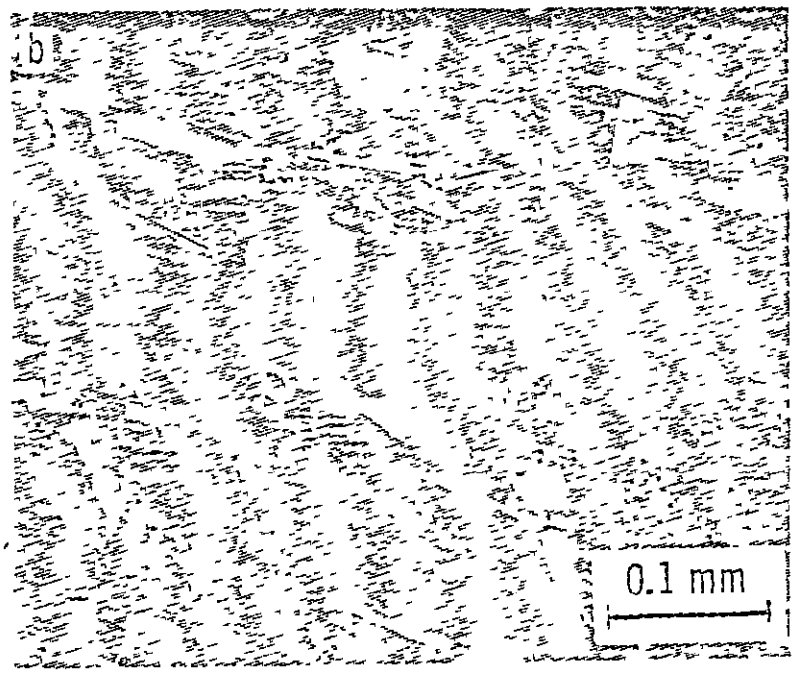

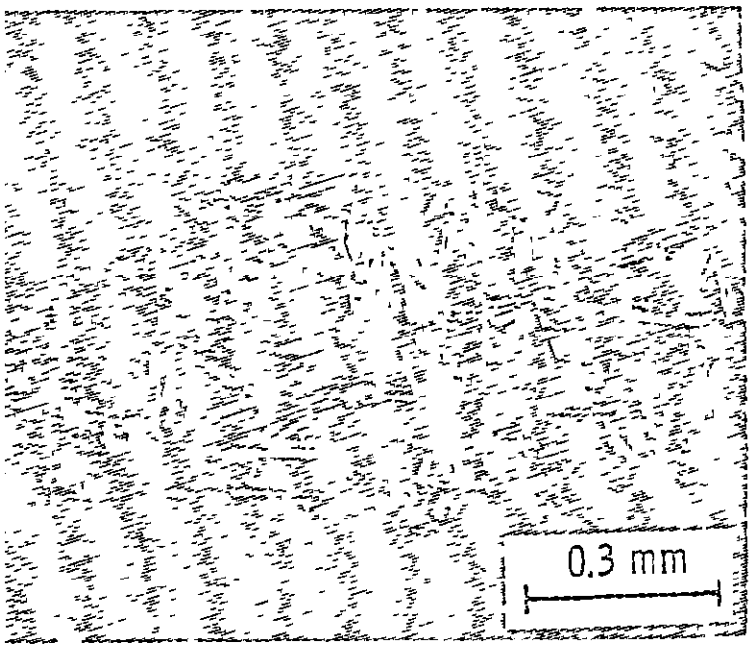

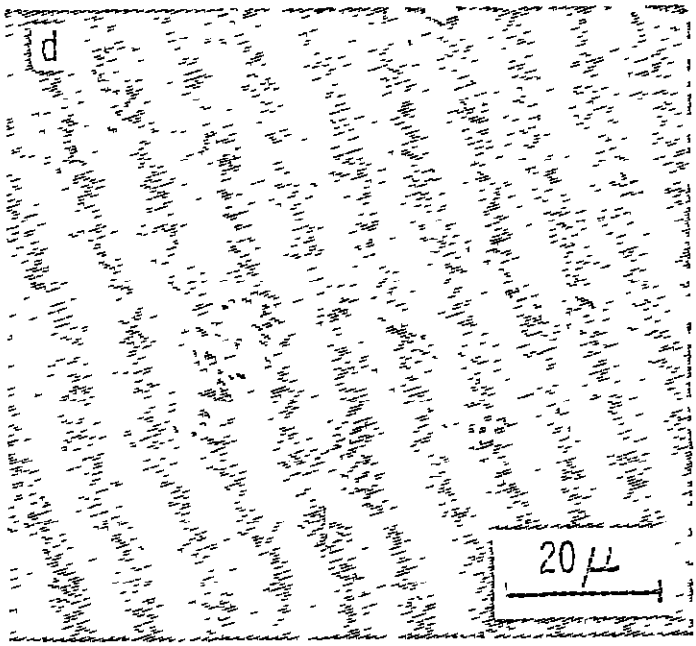

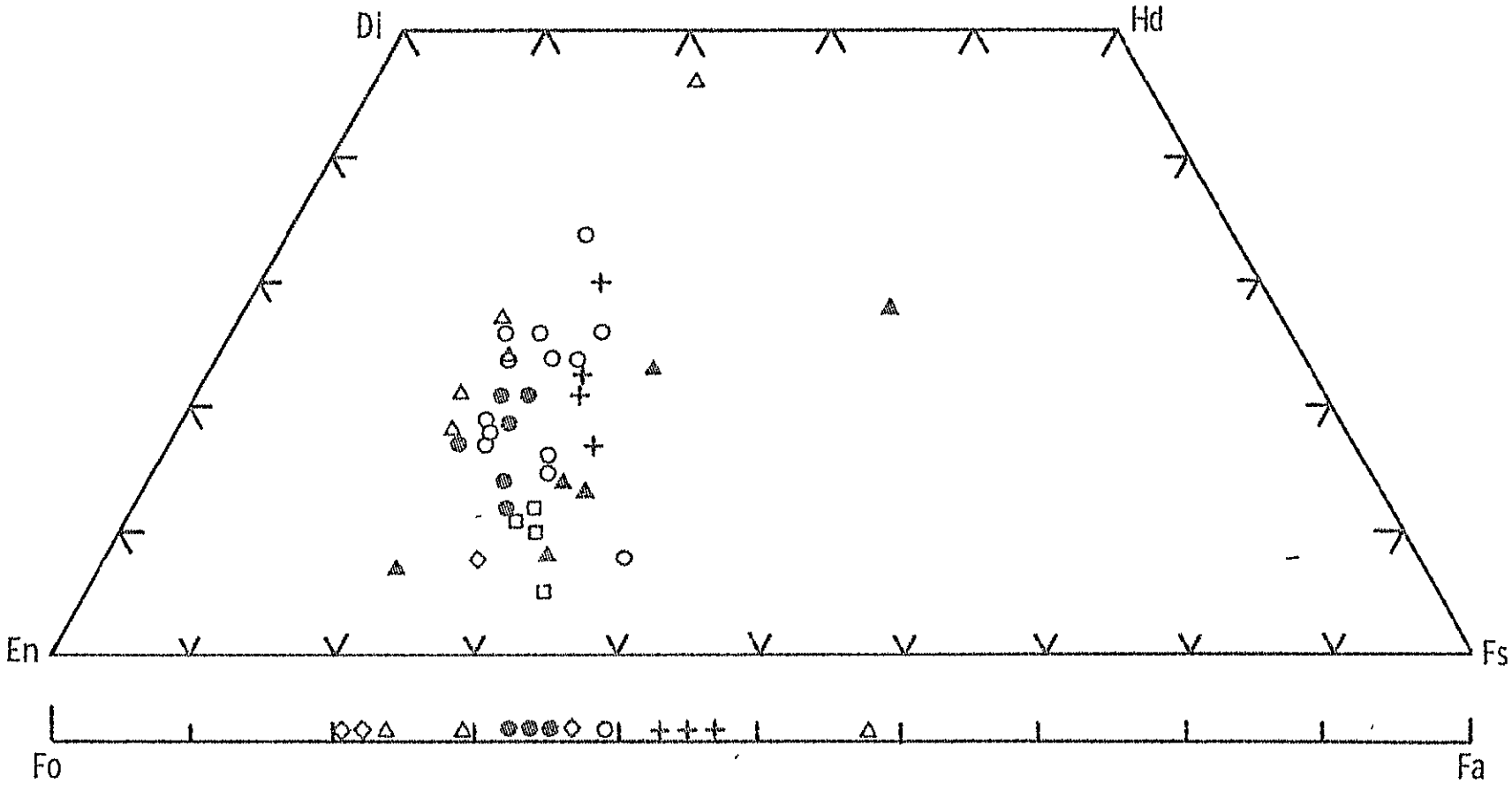
Di
Hd
En
Fs
Fo
Fa

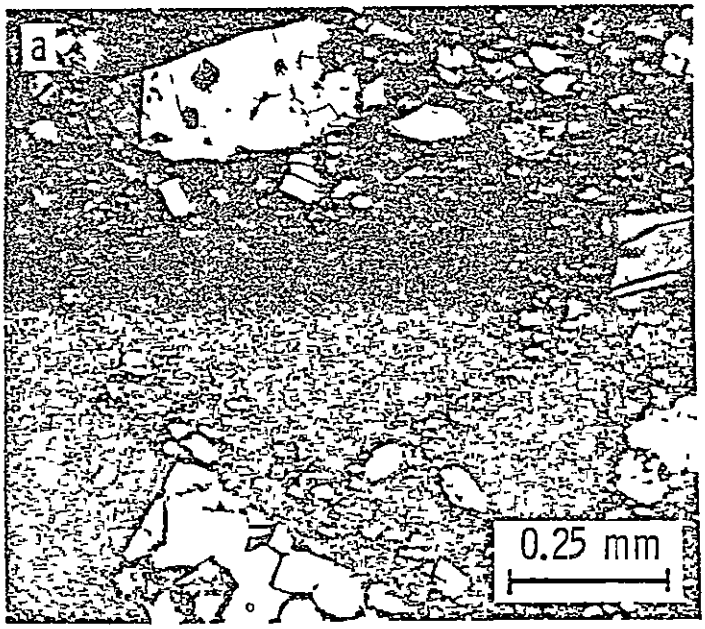

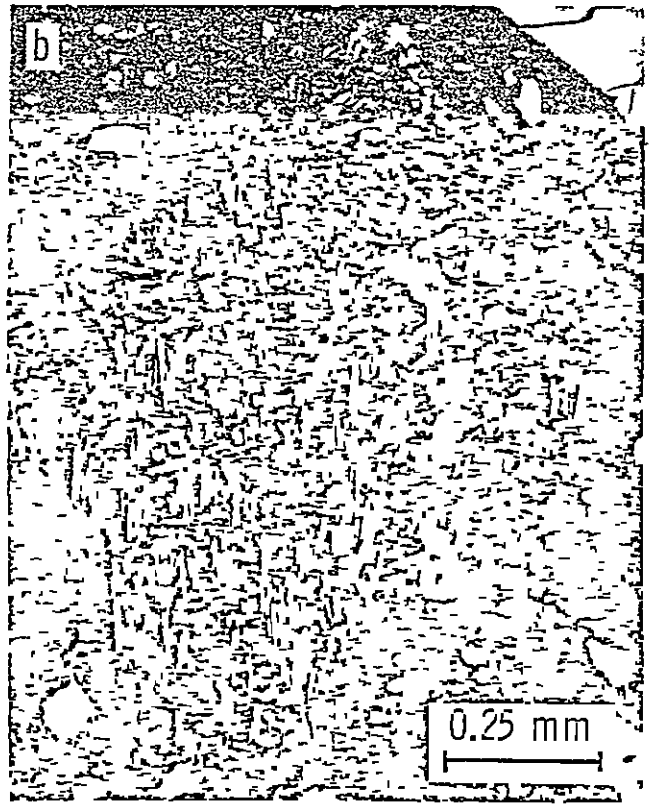

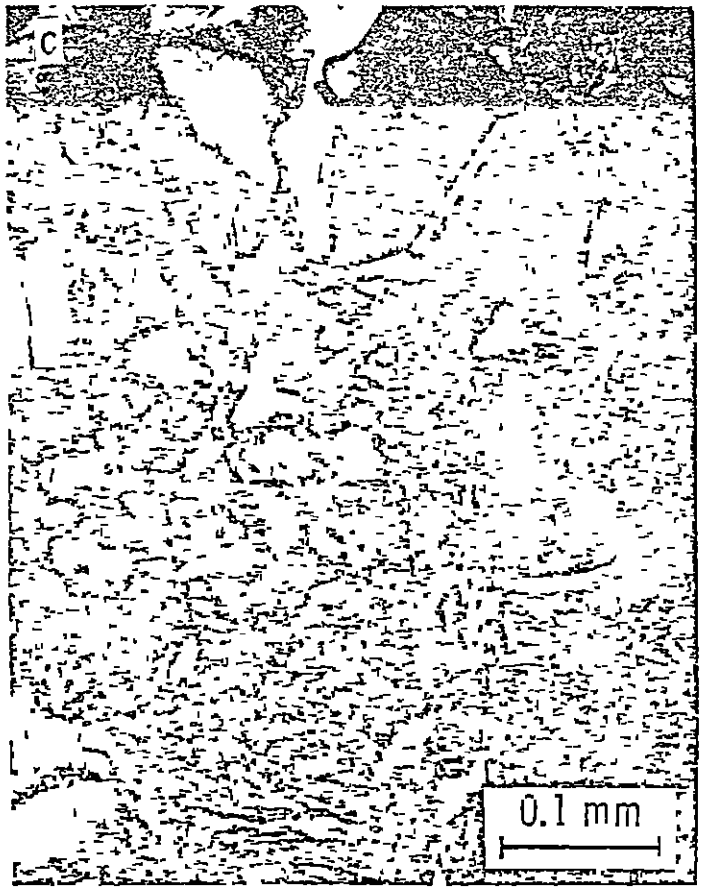

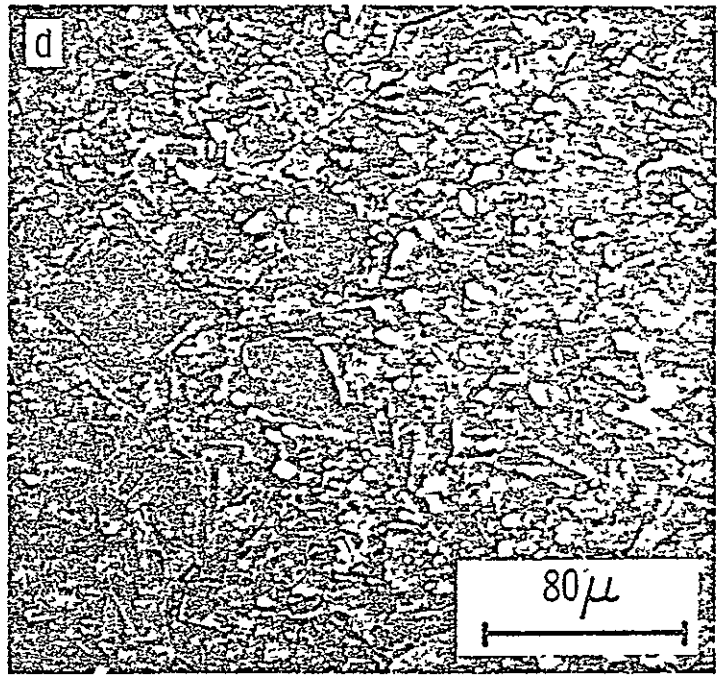

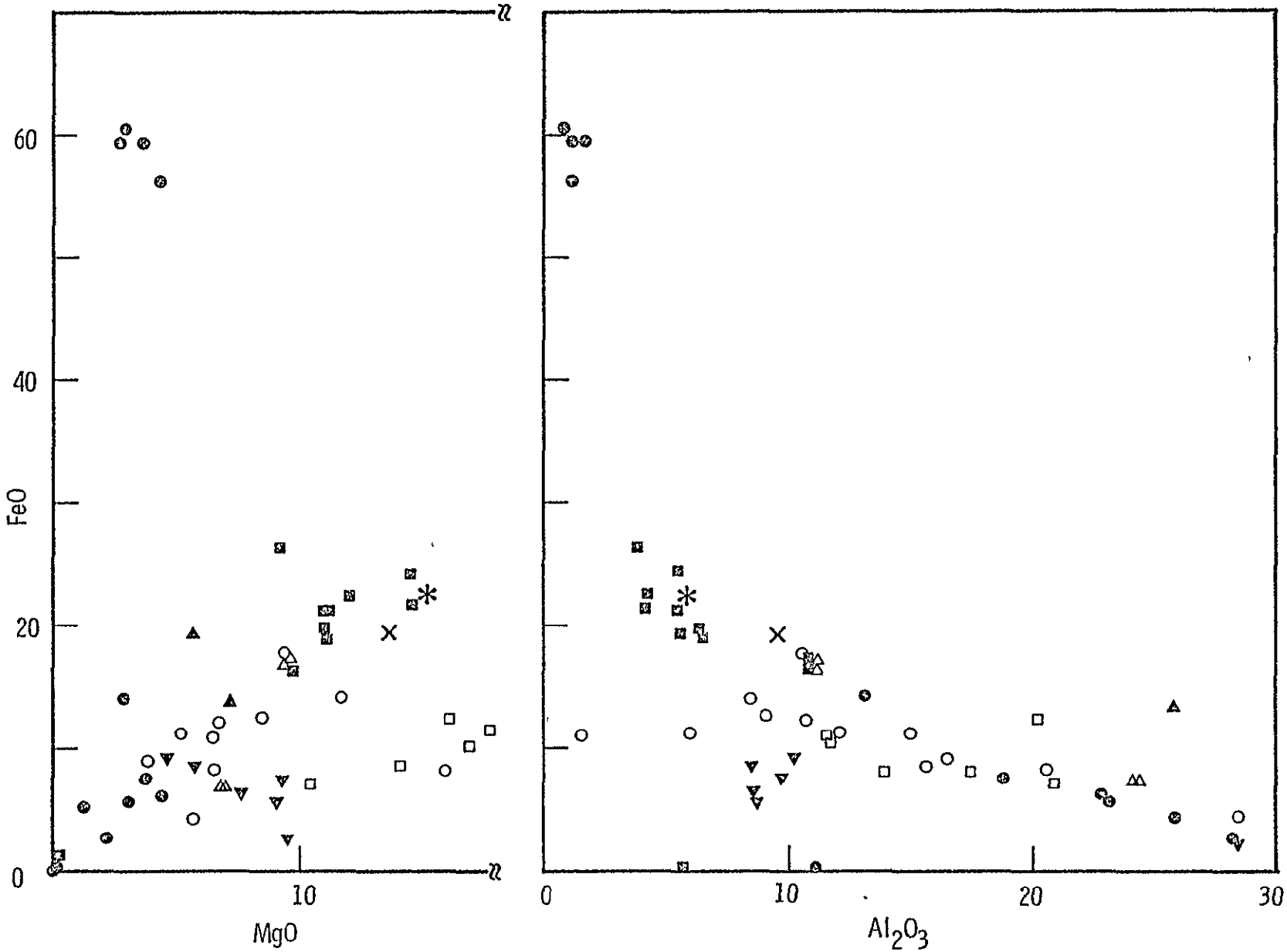
FeO
60
40
20
0
10
MgO
0
10
20
30
Al_2O_3

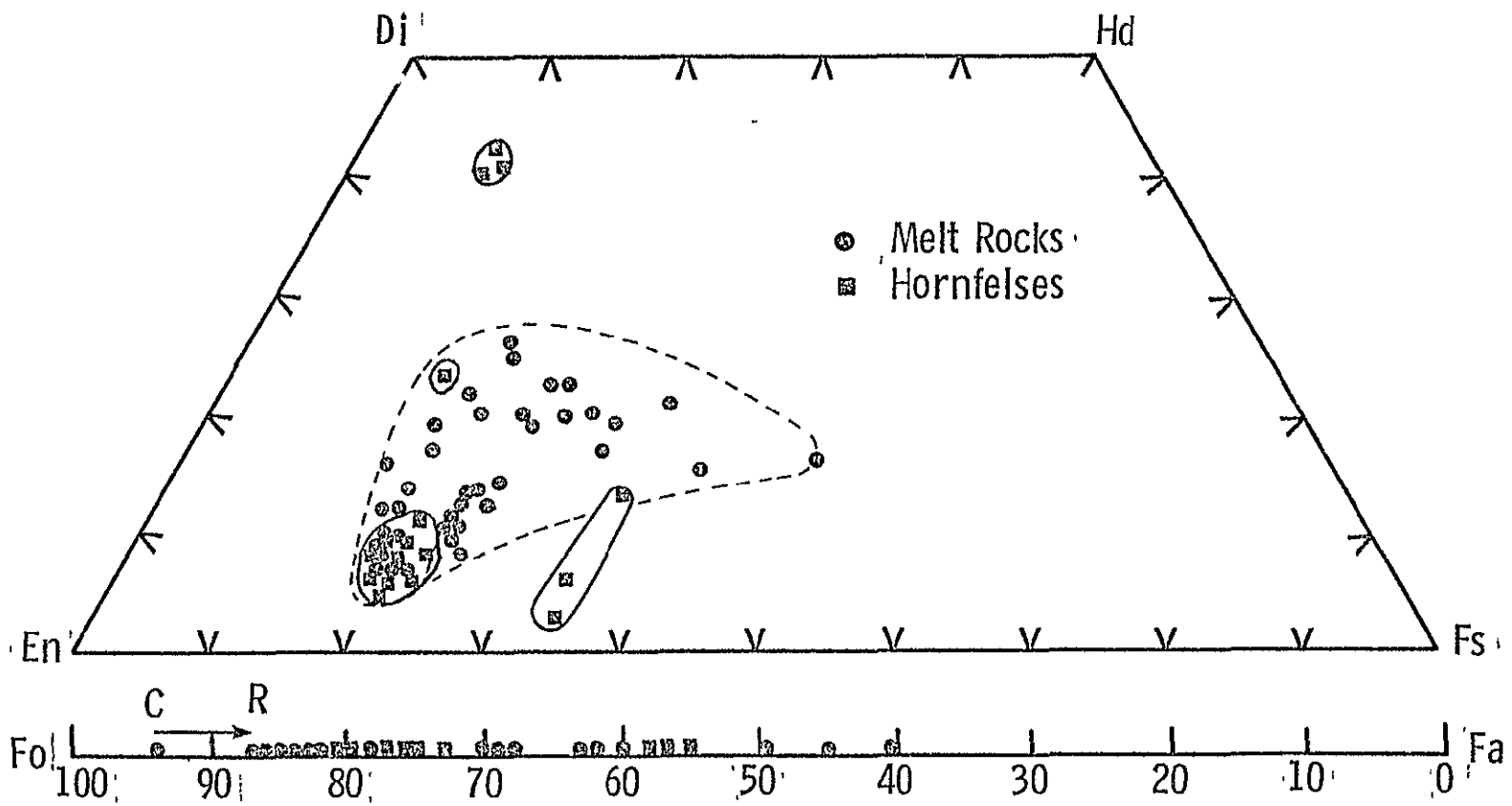

MELT ROCKS
HORNFELSES

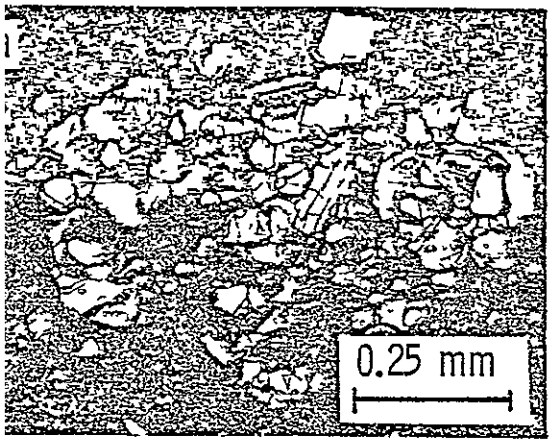

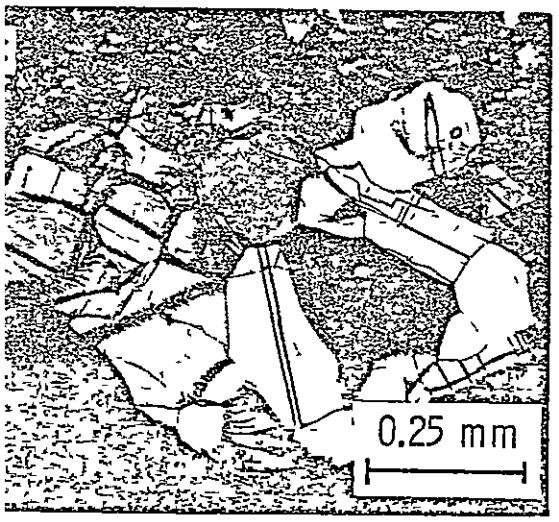

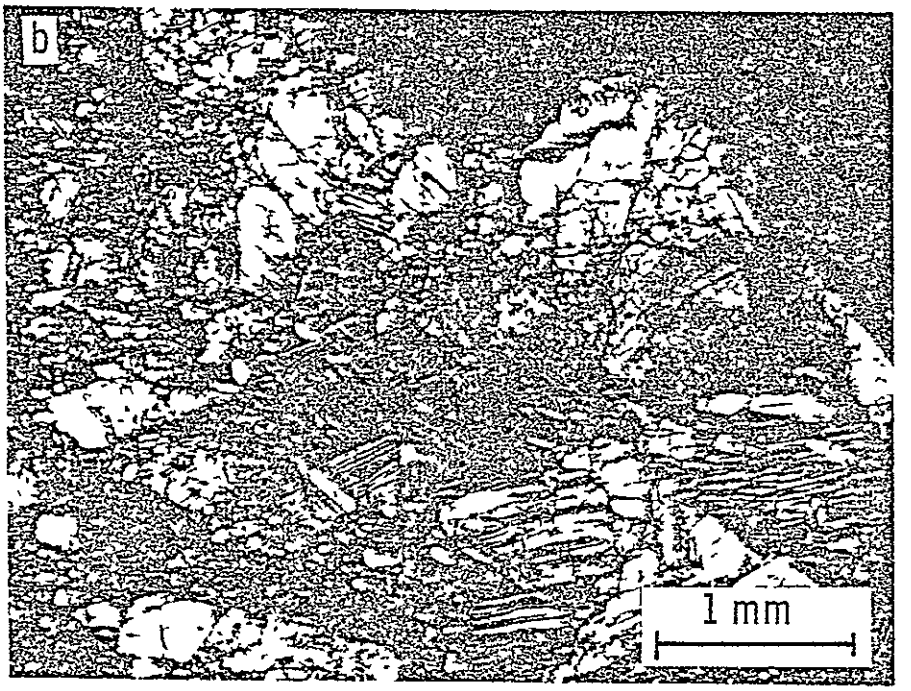

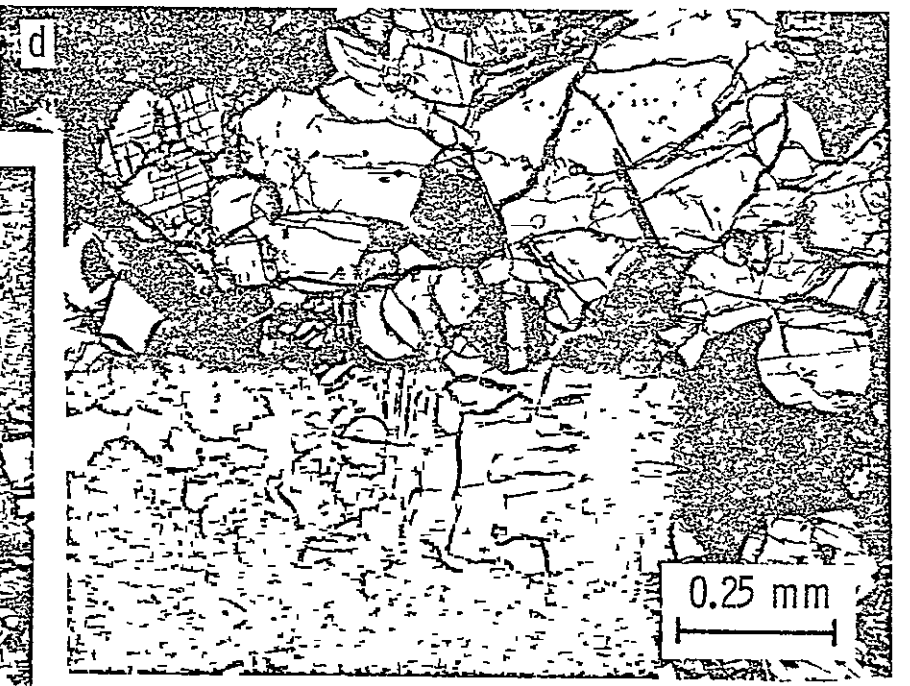

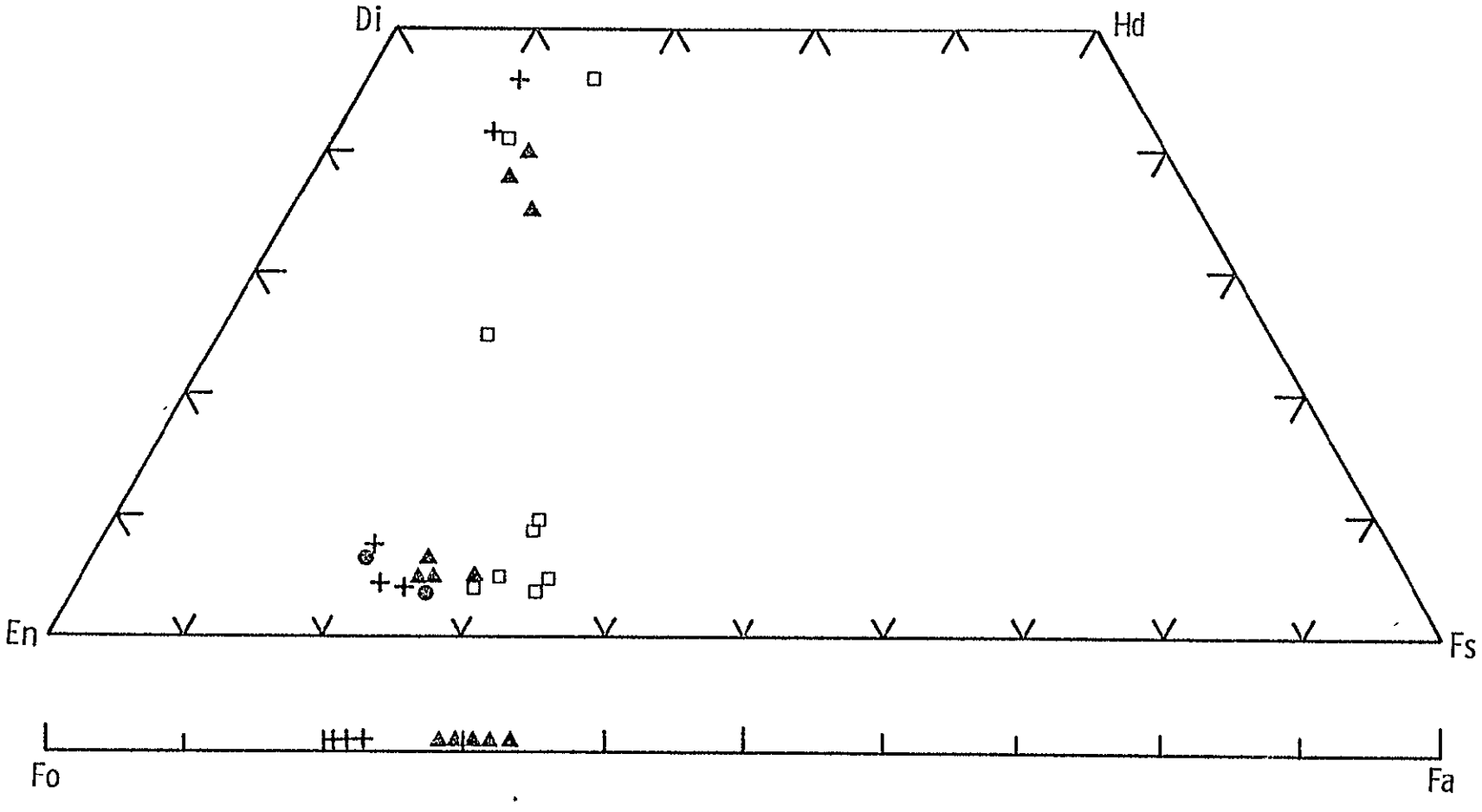
Di
Hd
En
Fs
Fo
Fa

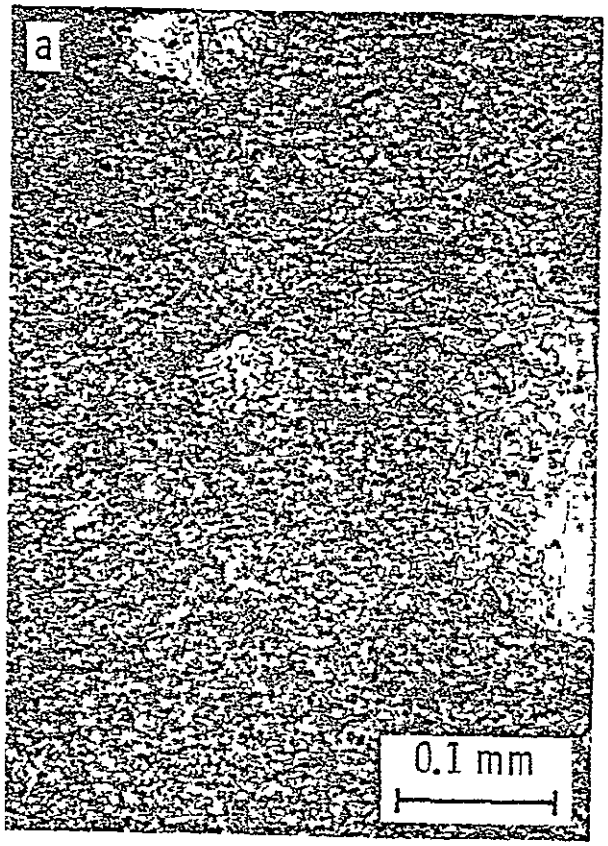

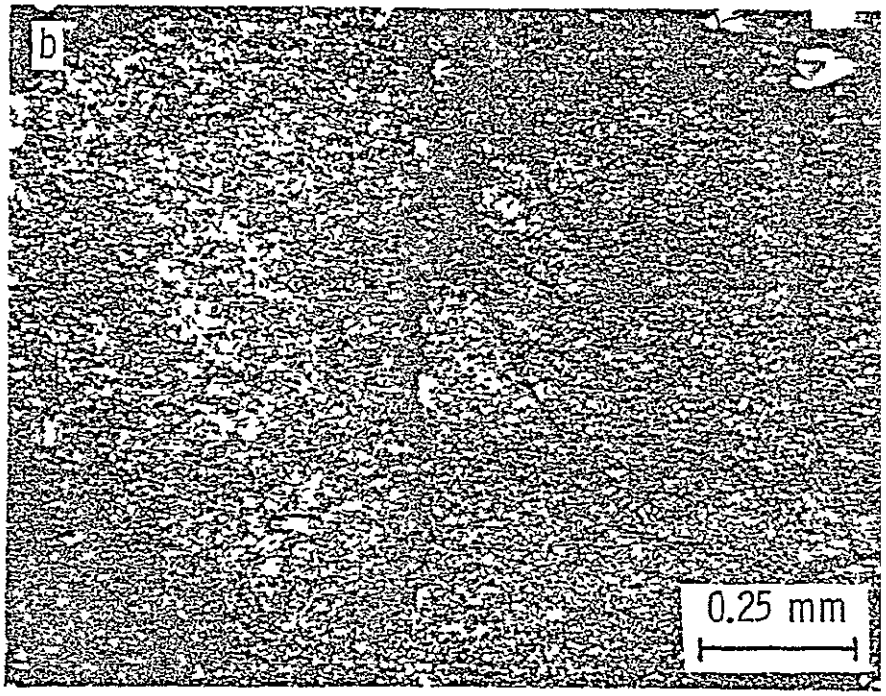

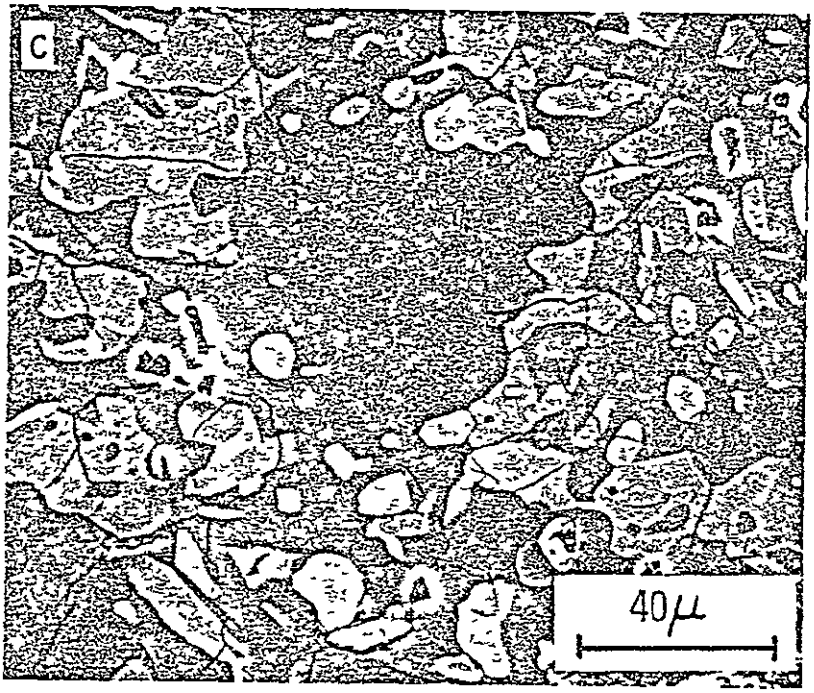

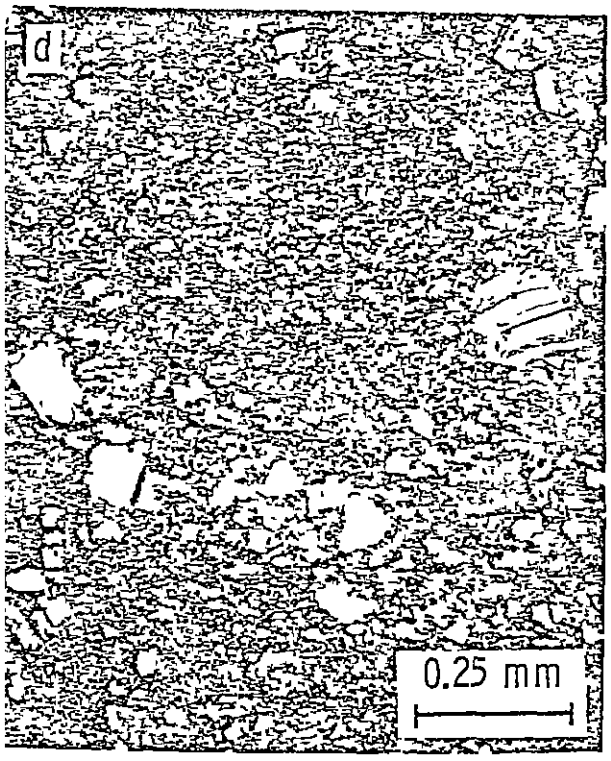

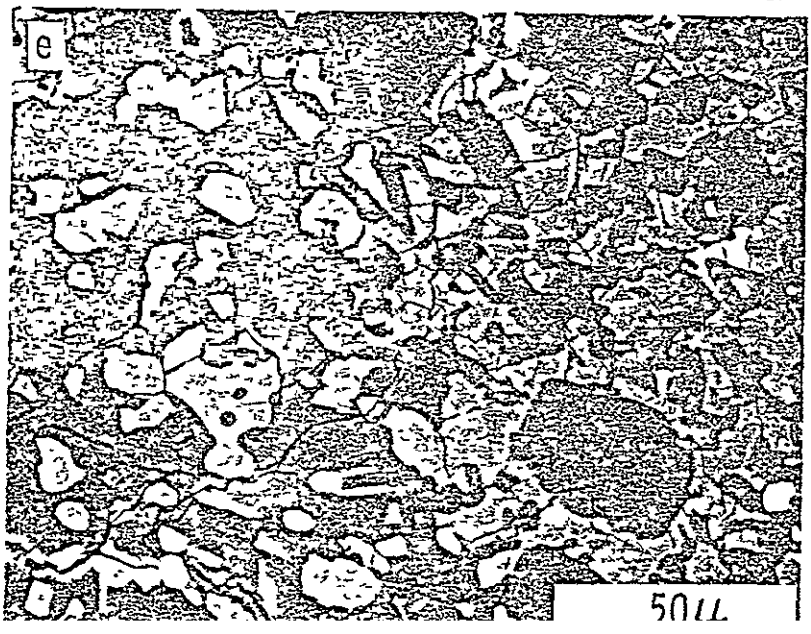

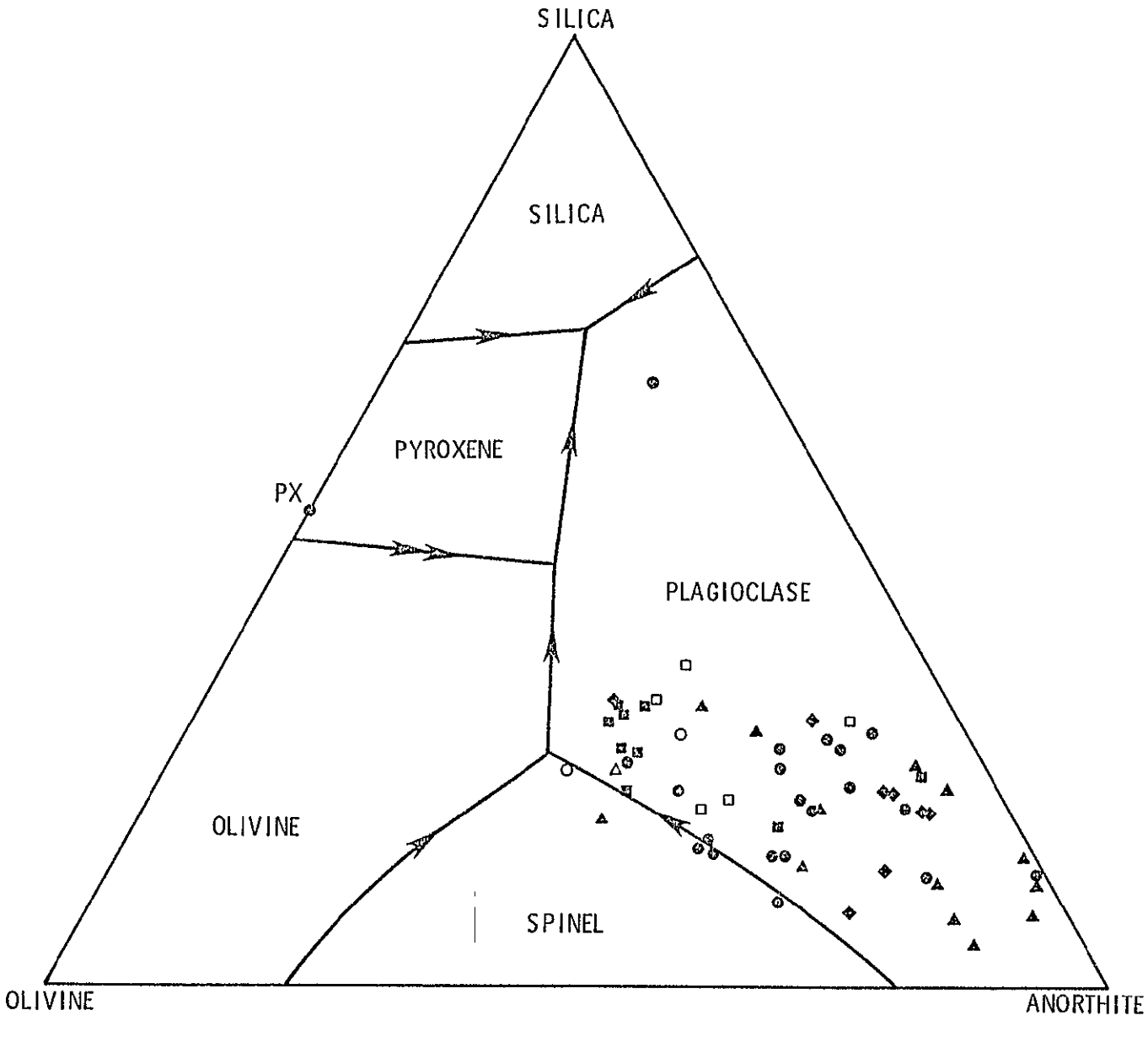
SILICA
SILICA
PYROXENE
PX
PLAGIOCLASE
OLIVINE
SPINEL
OLIVINE
ANORTHITE

Fig. 1 Photograph of 61175,19. This is the original slab, taken from the center of 61175. The large white clast is a moderately shocked anorthosite Smaller crystalline clasts are ANT and granulites, while the small dark grey clasts are impact melts or hornfelses. (NASA/JSC Photo 5-73-22080)

Fig. 2 SEM photomicrographs of polished thin sections of the matrix of 61175. a) Mineral fragments (mainly plagioclase) and small lithic fragments (lower right corner) in fine-grained groundmass. b) Higher magnification photo of relatively glass-free portion of the fine-grained matrix. Again, many of the fragments are plagioclase, but a small proportion in this size range are glass. c) Higher magnification photomicrograph of a more glass-rich portion of the matrix. These glassy areas interlock together to form a network which holds the rock together. Droplet chondrule in 61175 matrix. The chondrule is filled with plagioclase.

Fig. 3 Lithophile trace element abundances from clasts and matrix of 61175. 61175,133 and ,126 are dark clasts and are probably melt rocks. 61175,131 and ,170 are white clasts, and are moderately shocked anorthosites.

Fig. 4 Textures of "basalt" clasts a) Hyalocrystalline. Euhedral plagioclase laths (An_{95-97}) in random orientation in a glass matrix. The glass has a composition close to that of augite. b) Microdiabase porphyry. Phenocrysts of plagioclase in a groundmass of euhedral to subhedral plagioclase and subhedral pyroxene.

c) Typical basalt texture. Euhedral, tabular plagioclase phenocrysts (zoned $An_{97} \rightarrow An_{90}$) in a matrix of euhdral to subhedral plagioclase laths ($An_{90} \rightarrow An_{95}$), low calcium pyroxene ($Wo_{5-8}En_{71-73}Fs_{20-24}$) and olivine ($Fo_{77-78}$), glass and minor ilmenite. d) Scanning electron photomicrograph of a polished thin section of olivine basalt. This photomicrograph shows a typical mesostasis texture, containing pyroxene (darker gray), glass (lighter gray), ilmenite and Fe metal (bright spots).

Fig. 5 SEM/EDS analyses of pyroxenes and olivine from basalt clasts. Different symbols represent analyses of minerals from different clasts. Most points represent several analyses.

Fig. 6 Textures of melt-rocks from 61175. a) Maskelynite grain in matrix of 61175. b) Coarse-grained melt with intersertal texture. Plagioclase laths are aligned, indicative of flowage in the melt. Xenocrysts (longer subhedral to anhedral grains) of plagioclase ($\sim An_{95}$) and one small portion of an annealed xenolith (near the top of the clast) mark this as a melt rock. The melt matrix consists of plagioclase ($An_{83} \rightarrow An_{95}$, both zoned and unzoned) pyroxene ($Wo_5En_{59}Fs_{36}$), olivine (Fo_{72-75}) and glass. c) Fine grained, clast-laden melt rock. An annealed ANT clast (upper right) with a developing hornfels texture is enclosed in a fine grained matrix of plagioclase (An_{88-95}), pyroxene ($Wo_{17-31}En_{63-47}Fs_{18-20}$) and olivine ($Fo_{40-49}$). Pyroxenes with En contents as low as 33 also occur in this rock. These and the iron-rich olivines may be xenocrysts. d) Scanning electron photomicrograph of a metal-rich portion of a melt rock clast. Dark gray grains are phenocryst and groundmass

plagioclase, lighter grays are olivine, pyroxene and glass. Bright anhedral blebs are Fe metal with Ni contents of up to 9 wt.%, troilite and minor phosphide. Subhedral to euhedral lath-shaped grains are ilmenite.

Fig. 7 SEM/EDS analyses of glasses from melt-rocks and matrix of 61175. Different symbols indicate different clasts. *Composition of orange glass (74220) (Nava, 1974 Proc. Lunar Sci. Conf. 5th, 1087-1096) X Average Composition of Apollo 16 glasses, from Glass, 1976, Proc. Lunar Sci. Conf. 7th, 679-693. Filled circles represent glass from a breccia of mare basalt composition. The range of glass compositions is a result of differences in degree of crystallization, liquidus temperatures and crystallization histories of melt rocks found as clasts in 61175.

Fig. 8 SEM/EDS analyses of pyroxenes and olivines in melt-rocks and hornfelses from 61175.

Fig. 9 Textures of ANT suite clasts from 61175. a) Micro troctolite-granulite containing olivine (Fo_{77}), plagioclase (An_{95}) and minor low-Ca pyroxene (En_{70}). b) Shocked anorthosite; this is part of a large (~1 cm) brecciated clast. Some plagioclase has been partially transformed to maskelynite, other plagioclases show deformation lamellae (lower left). Very little glass is present. Plagioclase composition is An_{95}-An_{100}). c) Granulite. Anhedral plagioclase, with curving boundaries and triple-junctions is indicative of re-equilibration by subsolidus recrystallization. Subhedral orthopyroxene grain is located in the upper left corner. d) Norite granulite containing anhedral to subhedral

plagioclase, some slightly zoned (An_{97-95}). Anhedral orthopyroxene host ($Wo_4En_{63-67}Fs_{28-33}$) (lower left) encloses anhedral olivine. The bat shaped opaque mineral is a magnesian ilmenite. e) Poikiloblastic norite-granulite. A single large, anhedral orthopyroxene grain (at extinction) encloses anhedral to subhedral plagioclase (some with thin rims), anhedral olivine and anhedral to subhedral ilmenite. The groundmass (upper left) is granoblastic, and contains plagioclase, olivine and pyroxene.

Fig. 10 SEM/EDS analyses of pyroxenes from ANT suite rocks. Squares are mineral compositions from the clast shown in Fig. 6d, triangles from the clast shown in Fig. 6e. Most points represent several analyses.

Fig. 11 Textures of hornfelses from 61175. a) Granoblastic-hornfels consisting of olivine ($\sim Fo_{77}$), plagioclase ($\sim An_{95}$) and minor low Ca pyroxene. b) Unusual hornfelsed gabbro (?). This clast has mineral compositions distinct from all other hornfelses analyzed. Olivines (Fo_{55-58}) are more iron-rich than those from the other hornfelses (typically Fo_{74-80}) and the pyroxenes are also more iron-rich (En_{56-60}) than those of all other hornfelses (typically $\sim En_{75}$). c) Scanning electron photomicrograph of the texture of the hornfels shown in a. Anhedral plagioclase (dark gray) is surrounded by, and occasionally found as tiny inclusions in olivine (light gray). Curved boundaries show good triple junctions. Minerals are unzoned, and compositions vary only slightly throughout the clast. d) Poikiloblastic hornfels. Relatively large (.5-.7 mm) subhedral orthopyroxene poikiloblasts ($Wo_{4-8}En_{72-77}Fs_{18-20}$) enclose anhedral

to subhedral plagioclase ($\sim An_{88-90}$), subhedral plagioclase, xenocrysts and anhedral olivine (Fo_{78-81}). Interstitial material surrounding the pyroxene crystals is a granoblastic matrix of olivine and plagioclase (same composition as enclosed grains) with curved boundaries and triple-junctions. Larger, annealed xenocrysts are seen in the lower half of the clast. d) Scanning electron photomicrograph of the boundary between orthopyroxene poikiloblast and groundmass. The area of the photomicrograph is a portion of the lower boundary of the large orthopyroxene grain at the top of the clast in d. Note the anhedral to subhedral plagioclases and iron metal grains in the pyroxene (right half of the photograph) and the anhedral-granoblastic texture of the surrounding matrix (left half of photograph). The large orthopyroxene poikiloblasts contain irregular patches(?) of high calcium pyroxene ($Wo_{40-42}En_{48-50}Fs_{10-11}$). This texture, with the exception of grain size, is nearly the same as that of the granulite shown in Fig. 9e.

Fig. 12 Ternary diagram (after Walker, 1973b) of bulk compositions of clasts from 61175.

▲ ANT
▣ Hornfels
● Impact Melts
◆ Basalts

Unfilled symbols mark clasts whose classification is uncertain.

C.2